

An Automated EoS Tuning Procedure Using Global Optimization and Physical Constraints



An automated EoS tuning procedure using global optimization and physical constraints

by

Eirini-Maria Kanakaki

in partial fulfillment of the requirements for the degree of

Master of Science

in Petroleum Engineering

at the Technical University of Crete

Chania, February 2022

Supervisor:
Thesis committee:

Assistant Prof. Vassilis Gaganis,
Prof. Nikolaos Pasadakis,
Dr. Dimitris Marinakis,

NTUA
TUC
TUC



ΠΟΛΥΤΕΧΝΕΙΟ ΚΡΗΤΗΣ
TECHNICAL UNIVERSITY
OF CRETE

Acknowledgements

The completion of this Master Thesis could not have been possible without the supervision and assistance of Vassilis Gaganis, Assistant Professor at the National Technical University of Athens (NTUA). Therefore, I would like to take this opportunity and express my sincere and deepest gratitude to Professor Gaganis for his continuous support, patience, and countless sessions throughout this project. Under his supervision, I was introduced to how research works and I acquired valuable skills for my future endeavors.

I also owe a debt of gratitude to Nikolaos Pasadakis, Professor at the Technical University of Crete (TUC), for organizing this MSc program and giving me the opportunity to be mentored by established academics.

Finally, I would like to thank my parents for always supporting me to achieve my goals.

Eirini-Maria Kanakaki

Chania, February 2022

Abstract

The sampling process of petroleum fluids is a fundamental step in the development of a reservoir, as the subsequent laboratory PVT analysis provides a plethora of information regarding the thermodynamic behavior of a fluid. Due to the high cost of laboratory experiments, these are usually performed within a specific range of conditions (pressure and temperature) imposed by the reservoir itself. For this reason, a mathematical tool is required that can computationally predict the values of the required properties under a wide range of conditions expected to be encountered during the exploitation of the field both in the reservoir and in the wells. The most commonly used mathematical tool are the Equations of State (EoSs), the accuracy of which when applied to petroleum fluids is limited and can be optimized only if the equations are adjusted so that their predictions can adequately match the available measured PVT study values.

In this Master Thesis, the algorithms for simulating the Constant Composition Expansion test, the Differential Liberation test and the Separator test, which are performed to characterize reservoir fluids, were developed in the Matlab programming environment from scratch. It is important to mention that the key elements of the simulation of these PVT tests, which are the stability, flash and saturation pressure algorithms, were also developed in Matlab. The automated EoS tuning procedure was then performed using a global optimization method, the pattern search method, instead of a gradient-based method that does not always guarantee to find a global minimum and can get stuck at a local minimum. In addition, physical constraints increasing the physical soundness of the model's estimations were imposed. To test how efficient this approach is, one synthetic fluid and two real reservoir fluids were employed and the superiority of the pattern search method over the conventional gradient-based optimization method was confirmed.

TABLE OF CONTENTS

1. Introduction.....	13
1.1 Overview.....	13
1.2 Objective and structure of the Master Thesis	14
2. PVT Studies	15
2.1 Constant Composition Expansion (CCE)	17
2.2 Differential Liberation Expansion (DLE).....	19
2.3 Separator Test (ST).....	21
3. Simulation of PVT Studies	23
3.1 Stability Analysis	24
3.1.1 Michelsen’s graphical solution of the stability test.....	25
3.1.2 Michelsen’s algorithm	26
3.2 Flash Calculations.....	27
3.2.1 Mathematical approach of flash problem	28
3.2.2 Solving the system of $2N+1$ equations and $2N+1$ unknowns.....	29
3.3 Determination of saturation pressure.....	29
3.4 Simulation of PVT Experiments.....	30
3.4.1 Simulation of the Constant Composition Expansion test	30
3.4.2 Simulation of the Differential Liberation Expansion test.....	33
3.4.3 Simulation of the Separator Test.....	36
4. Cubic Equations of State.....	37
4.1 Peng-Robinson cubic Equation of State (PR EoS)	37
4.2 Critical properties and acentric factor.....	38
4.3 Mixing rules and binary interaction coefficients	40
4.4 Volume shift.....	40
4.5 Lumping and delumping method	41

5.	Tuning Methodology	43
6.	Optimization	45
6.1	What is optimization?	45
6.2	Pattern search method	46
6.3	Development of the objective function and pattern search implementation for EoS tuning.....	48
7.	Results.....	49
7.1	Four-component synthetic mixture	49
7.1.1	First Case Scenario – Synthetic mixture.....	50
7.1.2	Second Case Scenario – Synthetic mixture	51
7.1.3	Third Case Scenario – Synthetic mixture	52
7.1.4	Fourth Case Scenario – Synthetic mixture.....	53
7.1.5	Fifth Case Scenario – Synthetic mixture	54
7.1.6	Sixth Case Scenario – Synthetic mixture.....	55
7.2	Real reservoir fluid 1	56
7.3	Real reservoir fluid 2	60
8.	Conclusions.....	70

LIST OF TABLES

Table 3.1: Michelsen’s algorithm results.....	27
Table 7.1: Composition of the four-component synthetic mixture.....	49
Table 7.2: Optimized value of P_c (MPa) in the first case scenario.	50
Table 7.3: Optimized value of BIC in the second case scenario.	51
Table 7.4: Optimized value of the T_c of third and fourth component in the third case scenario.	52
Table 7.5: Optimized value of ω of third and fourth component in the second case scenario.	53
Table 7.6: Optimized value of critical temperature of the second, third and fourth component in the fifth case scenario.....	55
Table 7.7: Optimized value of the critical pressure, the critical temperature and the acentric factor of the fourth component in the sixth case scenario.....	55
Table 7.8: Composition of the real reservoir fluid 1 before split and lump.....	56
Table 7.9: Results received after the tuning process before splitting and lumping of the C_{12+}	57
Table 7.10: First case scenario.....	58
Table 7.11: Third case scenario.	58
Table 7.12: Fourth case scenario.	59
Table 7.13: Sixth case scenario.....	59
Table 7.14: Composition of the real reservoir fluid 2 after split and lump.	60
Table 7.15: Saturation pressure after the optimization process.	61
Table 7.16: Separator Test Results.	69

LIST OF FIGURES

Figure 2.1: The typical route that a petroleum fluid follows from the reservoir to ambient conditions (Pedersen & Christensen, 2007).....	16
Figure 2.2: Schematic description of a constant composition expansion test for an oil sample (Pedersen & Christensen, 2007).	18
Figure 2.3: Relative volume versus pressure for determination of saturation pressure from CCE data (Σταματάκη & Αυλωνίτης, 2004).....	19
Figure 2.4: Schematic illustration of the Differential Liberation Expansion test (Pedersen & Christensen, 2007).	20
Figure 2.5: Schematic representation of a three-stage separator experiment (Pedersen & Christensen, 2007).	21
Figure 3.1: Tuning process of Equations of State.....	23
Figure 3.2: Michelsen’s graphical solution of the stability test. (Whitson, 2000).....	25
Figure 3.3: Schematic depiction of a flash cell (Pedersen, 1989).....	28
Figure 3.4: Flow diagram of the simulation of the Constant Composition Expansion test.....	32
Figure 3.5: Flow diagram of the simulation of the Differential Liberation Expansion test.....	35
Figure 3.6: Flow diagram of the simulation of the Separator Test.	36
Figure 4.1: Estimation path of the molar volume of pure components.	39
Figure 6.1: Minimum of $f(x)$ is same as maximum of $-f(x)$	45
Figure 6.2: Example of successful poll (www.mathworks.com).....	47
Figure 6.3: Example of unsuccessful poll (www.mathworks.com).....	48
Figure 7.1: Total Error vs P_c of 4 th component – Synthetic mixture.	50
Figure 7.2: Total Error vs k_{ij} of CH_4 and C_{20} – Synthetic mixture.	51
Figure 7.3: Contour plot of the 2D optimization problem of the third case scenario. .	53
Figure 7.4: Contour plot of the 2D optimization problem of the fourth case scenario.	54
Figure 7.5: Relative Volume vs Pressure.....	62
Figure 7.6: Isothermal Compressibility vs Pressure.	63
Figure 7.7: B_o vs Pressure.	64
Figure 7.8: R_s vs Pressure.	65
Figure 7.9: Oil density vs Pressure.	66

Figure 7.10: Z factor vs Pressure.	67
Figure 7.11: S_g vs Pressure.	68

1. Introduction

The introduction chapter serves two main purposes. The first section of this chapter aims at highlighting the importance of tuning the Equation of State (EoS) models used in compositional reservoir simulation to predict the phase behavior of petroleum reservoir fluids, whereas the last section of the chapter presents the main objective and structure of this Master Thesis. In essence, this chapter introduces the complex topic of EoS tuning so that the following chapters can be better understood.

1.1 Overview

Equation of State (EoS) models are fluid models that are used extensively in Petroleum Engineering for the reservoir dynamic simulation process. More precisely, EoSs are thermodynamic expressions that relate the pressure (P), the volume (V), the temperature (T) and the composition (z) of a reservoir fluid system. These mathematical models stem from the Ideal Gas Law and make use of compositional and characterization laboratory data of reservoir fluids for their development. The calculated molar volume (V_m) is used for the determination of more complex thermophysical properties as well as for the specification of the thermodynamic equilibrium.

In the oil and gas industry, cubic Equation of State (cEoS) models, such as the Peng-Robinson Equation of State (PR EoS) ones, are the most commonly used as they are among the most computationally efficient EoSs. However, cEoSs cannot be used as predictive models because their relatively simplistic approach of the physical phenomena and the uncertainties in the molecular weight and critical properties of the heavy fraction of the hydrocarbon mixtures render them as non-predictive models, that is they are insufficient to accurately simulate the phase and volumetric behavior of reservoir fluids under various conditions. Therefore, tuning of EoS models comprises a significant prerequisite for the provision of accurate predictions. Tuning of EoSs is basically a procedure during which the parameters of the poorly defined components of a hydrocarbon mixture of a cEoS model are adjusted such as that the difference between the available experimental data and the predictions generated by the cEoS model is minimized.

1.2 Objective and structure of the Master Thesis

The main focus of this Master Thesis is the proposal of a method for guiding the tuning procedure of the PR EoS model against a set of laboratory data, which were generated in PVT laboratories at specific pressures and temperatures, so as to increase accuracy and to enhance the physical soundness of the tuned PR EoS. All routine PVT experiments were simulated using the Matlab programming environment and the PR EoS tuning was performed using a derivative-free global optimization method, the pattern search one. One synthetic and two real petroleum fluids were employed.

The Master Thesis is developed as follows:

- Chapter 2 provides a description of the three main PVT experiments designed to study and quantify the phase behavior and properties of reservoir fluids.
- Chapter 3 describes how these PVT studies can be simulated by means of an EoS model.
- Chapter 4 introduces the PR cEoS as well as the requirements this model must fulfill in order to be used as a computational tool in petroleum systems.
- Chapter 5 discusses the tuning methodology used in this Master Thesis.
- Chapter 6 explains what optimization is and provides details regarding the pattern search optimization method.
- Chapter 7 discusses the results obtained after the tuning process of the sample fluids.
- Chapter 8 presents the conclusions of this Master Thesis and demonstrates the success of the developed method.

2. PVT Studies

As already mentioned in Chapter 1, an essential part of tuning an EoS model is carrying out PVT experiments at specific pressures and temperatures in the laboratory in order to determine the phase behavior and fluid properties of petroleum fluid samples. This chapter discusses thoroughly the main three PVT tests studied in this Master Thesis.

The acquisition of accurate and reliable data regarding the volumetric properties and phase equilibrium of the reservoir fluids is essential for the hydrocarbon recovery to be optimized. This information is required for the estimation of the reserves, the optimal development and production design of the reservoir as well as the determination of the quantity and quality of the produced fluids. During hydrocarbon extraction, reservoir pressure decreases as reservoir fluids are recovered, whereas the temperature within the reservoir remains constant provided that no thermal Enhanced Oil Recovery (EOR) technique is applied. Therefore, the pressure of the subsurface reservoir is the primary variable that determines the thermodynamic behavior of reservoir fluids, under reservoir conditions, during oil and gas production. The volumetric and phase changes the reservoir fluid undergoes on its way (Figure 2.1) from the reservoir to the production wells and finally to the surface at standard conditions (60 °F, 14.7 psia), can be studied in a PVT lab by simulating what takes place within the petroleum reservoir and at surface during production.

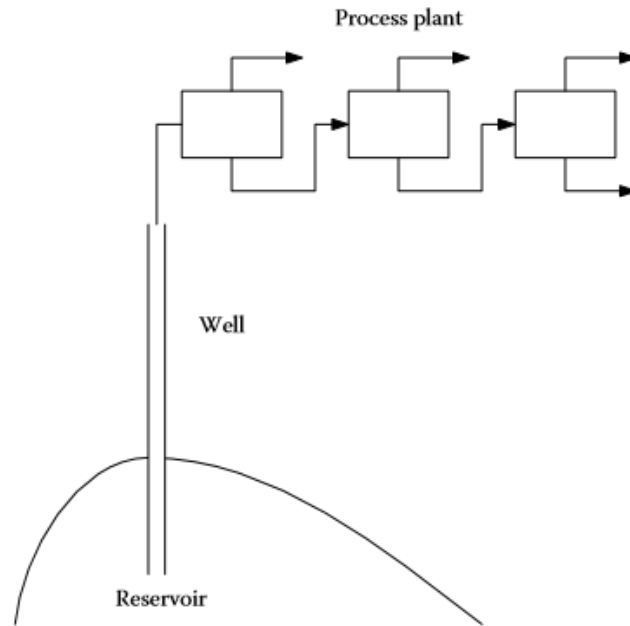


Figure 2.1: The typical route that a petroleum fluid follows from the reservoir to ambient conditions (Pedersen & Christensen, 2007).

The volumetric and phase changes that take place in a reservoir, during its trip through the reservoir, well and process plant, can be studied by performing PVT experiments on a reservoir fluid sample. The following laboratory measurements and tests are routinely conducted to characterize adequately a reservoir fluid during the first stages of the development and production of the hydrocarbon field. These tests include:

- Compositional Analysis
- Constant Composition Expansion (CCE)
- Differential Liberation Expansion (DLE)
- Constant Volume Depletion (CVD)
- Separator Test (ST)
- Viscosity Study (VS)

In this Master Thesis, the following three PVT tests were employed:

- Constant Composition Expansion (CCE)
- Differential Liberation Expansion (DLE)
- Separator Test (ST)

This section describes thoroughly these three PVT tests. The CVD experiment was skipped since no gas condensate mixture was used in this Master Thesis. In addition,

the VS is not described because of the fact that the viscosity of a fluid cannot be computed using an Equation of State that aims to model the volumetric, not the kinetic, behavior of a reservoir fluid. At this point, it should be reminded that the information in this chapter was used in the following chapters for the tuning process of the PR EoS, which is the topic of this Master Thesis.

2.1 Constant Composition Expansion (CCE)

The saturation pressure, which is the pressure at which the second phase of a petroleum fluid at some reference temperature (reservoir temperature) first appears in an infinitesimal quantity, is determined during the Constant Composition Expansion or Constant Mass Expansion test (CCE). The saturation pressure corresponds either to a bubble point (P_b) or dew point (P_d) based on the nature of the collected reservoir fluid sample. In addition, during the CCE test it is possible to determine the volumetric behavior of the two phases of the fluid at pressures below the saturation one. It is worth mentioning that during this test no gas or liquid phase is removed from the cell.

Initially, the hydrocarbon fluid sample (oil or gas) is placed in a visual PVT cell at reservoir temperature and at a pressure in excess of the initial reservoir pressure. For an oil mixture this means that the experiment commences at a pressure above the bubble point and for a gas mixture this means that the experiments starts at a pressure above the dew point. The initial volume of the mixture is recorded. The pressure is reduced in steps at constant temperature and the change in the total hydrocarbon volume (V_t) is measured at each pressure step. The saturation pressure (bubble point or dew point) and the corresponding volume are observed, recorded and used as a reference volume (V_{sat}). The volume of the hydrocarbon system, which is a function of the cell pressure, is reported as its ratio over the reference volume.

Figure 2.2 depicts schematically the CCE experiment as described above.

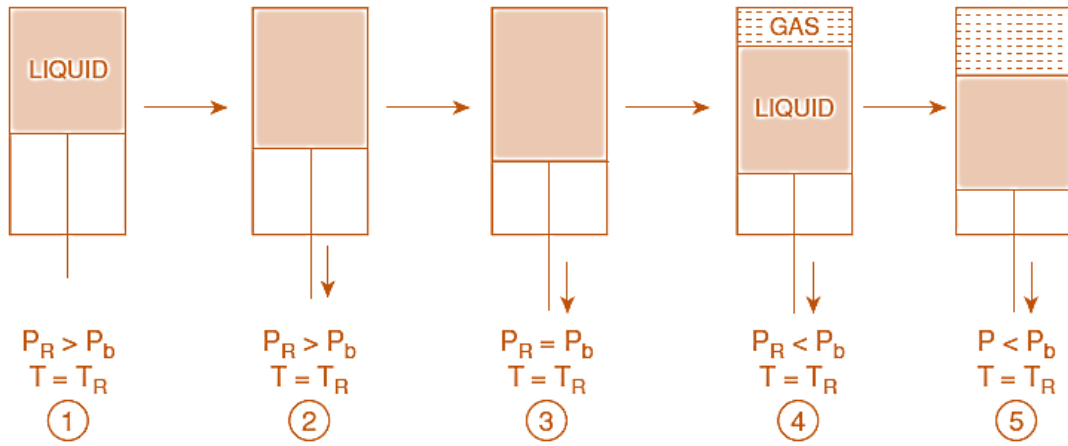


Figure 2.2: Schematic description of a constant composition expansion test for an oil sample (Pedersen & Christensen, 2007).

The properties that are determined during the CCE test at each pressure step are the relative volume (V_r) and the isothermal compressibility (c).

- Relative volume (V_r)

It is the ratio of the total fluid volume to the saturation volume and equals to one at P_{sat} .

$$V_r = \frac{V}{V_{sat}} \quad (2.1)$$

- Isothermal compressibility (c_o) (it is only reported for pressures above the saturation pressure where the fluid is monophasic)

$$c_o = -\frac{1}{V_r} \left[\frac{\partial V_r}{\partial P} \right]_T \quad (2.2)$$

Figure 2.3 depicts a typical plot of relative volume versus pressure, which results from the Constant Composition Expansion test, in which the bubble saturation pressure can be detected due to the slope discontinuity that can be observed.

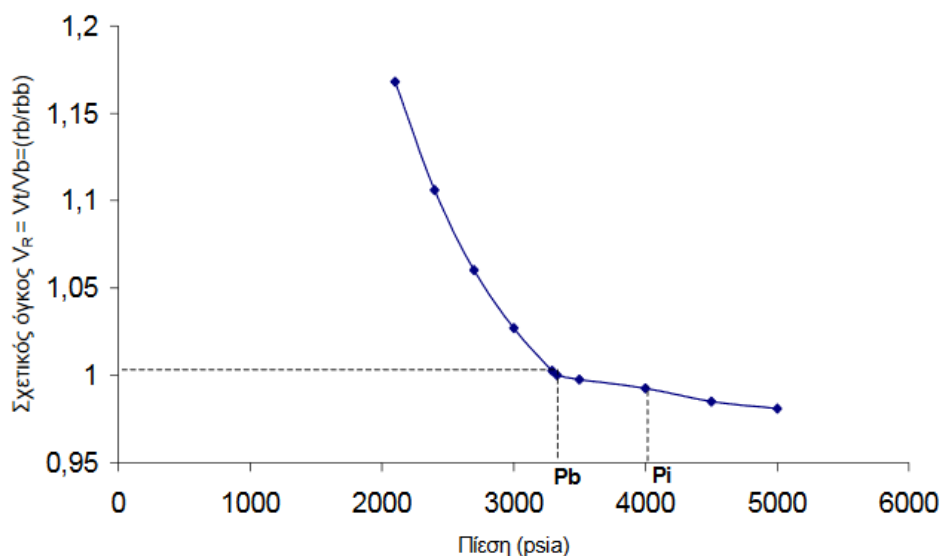


Figure 2.3: Relative volume versus pressure for determination of saturation pressure from CCE data (Σταματάκη & Αβλωνίτης, 2004).

2.2 Differential Liberation Expansion (DLE)

The main purpose of the Differential Liberation Expansion or Differential Vaporization test (DLE) is the description of the separation-process taking place within the petroleum reservoir and the laboratory simulation of the flowing behavior of hydrocarbon systems at conditions above the critical gas saturation. This PVT experiment is usually carried out for black and volatile oils.

As depicted in Figure 2.4, the oil sample is equilibrated in a PVT cell at its bubble point pressure and at temperature equal to the reservoir one. The pressure inside the cell is reduced stepwise by increasing its volume, which results in the formation of a gas phase since the cell pressure is less than the bubble point pressure. The gas is equilibrated with the liquid in the cell by agitation. Once equilibrium has been established between the gas and fluid phase and once the values of pressure and volume have been recorded, the gas is completely displaced from the cell at constant pressure by slowly reducing the volume of the cell, which causes the overall composition of the oil sample to change. Usually, the DLE test continues until the pressure becomes equal to the ambient pressure before cooling off the cell to 15°C (or standard).

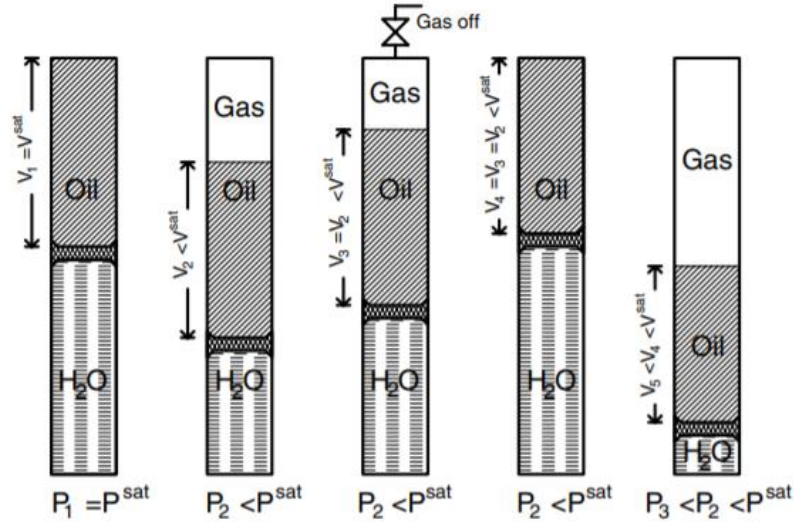


Figure 2.4: Schematic illustration of the Differential Liberation Expansion test (Pedersen & Christensen, 2007).

The properties that are determined by the DLE test are the following:

- B_o (Oil Formation Volume Factor)

It is the volume in barrels (rb) ($V_{o\ rc}$) of the oil at each pressure step to the volume of oil at the final stage of the process ($V_{o\ sc}$), which is known as the residual oil:

$$B_o = \frac{V_{o\ rc}}{V_{o\ sc}} \left(\frac{\text{rb}}{\text{stb}} \right) \quad (2.3)$$

- R_s (Solution Gas-Oil Ratio, GOR)

It is the volume of the cumulative gas ($V_{g\ sc}$) (measured at sc) to the volume of the residual oil:

$$R_s = \frac{V_{g\ sc}}{V_{o\ sc}} \left(\frac{\text{scf}}{\text{stb}} \right) \quad (2.4)$$

- Specific Gravity of Oil ($S_{g,\text{oil}}$)

It is determined as the density of oil at each pressure step to the density of water at 60 °F.

$$S_{g,\text{oil}} = \frac{\rho_{\text{oil\ rc}}}{\rho_{\text{water (60°F)}}} \quad (2.5)$$

- Compressibility factor (Z)

The compressibility factor is a liberated gas phase property and can be determined by the gas equation.

$$PV = nZRT \rightarrow Z = \frac{PV}{nRT} \quad (2.6)$$

- Specific Gravity of Gas ($S_{g, \text{gas}}$)

It is determined as the density of gas liberated at each pressure step to the density of air at 60 °F.

$$S_{g, \text{gas}} = \frac{\rho_{\text{gas sc}}}{\rho_{\text{air}(60^\circ\text{F})}} \quad (2.7)$$

2.3 Separator Test (ST)

The two PVT experiments mentioned so far are only related to the PVT behavior of petroleum fluids under reservoir conditions.

The separator experiments are carried out either for oil or gas mixtures. The primary purpose of these experiments is the determination of the number of the required separation stages at surface as well as of the conditions (pressure and temperature) at which the separators should operate in order for the production to be optimized. For an oil reservoir, the optimization of the production is achieved when the gas production decreases and the oil production is maximized (obtain a minimum GOR value). Generally, two or three separators are employed, and the final separation in the last separator (tank) takes place at ambient pressure and temperature conditions.

A three-stage separator test is sketched in Figure 2.5.

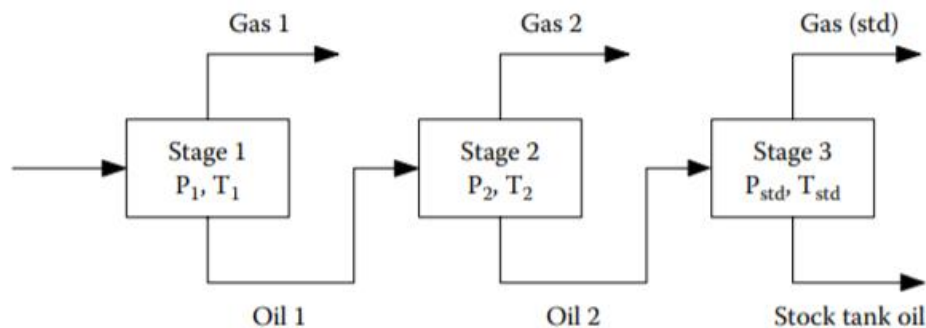


Figure 2.5: Schematic representation of a three-stage separator experiment (Pedersen & Christensen, 2007).

The primary results from a separator experiment performed on a gas condensate mixture or an oil system are the following:

- Separator GOR (Gas-Oil Ratio)

It is the volume of gas from actual separator stage at standard conditions divided by the volume of the oil from the last stage (at atmospheric conditions).

$$\text{GOR} = \frac{V_{g\ sc}}{V_{o\ sc}} \left(\frac{\text{scf}}{\text{stb}} \right) \quad (2.8)$$

- API gravity of tank oil

$$\text{API} = \frac{141.5}{S_{g,\text{oil}}} - 131.5 \quad (2.9)$$

- Separator B_o (Oil Formation Volume Factor)

It is the volume of oil at actual separator stage to the volume of oil from last stage (atmospheric conditions).

$$B_o = \frac{V_{o\ rb}}{V_{o\ sc}} \left(\frac{\text{rb}}{\text{stb}} \right) \quad (2.10)$$

In general, this test's results are used to adjust DLE data against the surface separator train.

3. Simulation of PVT Studies

The PVT experiments mentioned in Chapter 2 study and quantify the phase behavior and properties of reservoir fluids at specific temperatures and pressures. For this reason, the simulation of these PVT studies is required to predict the values of the required properties under a wide range of conditions expected to be encountered during the exploitation of the field both in the reservoir and in the wells. The mathematical tools used to simulate these PVT studies are the EoSs. As mentioned in the introductory chapter, the tuning of an EoS model is necessary in order accurate estimations of thermodynamic properties and derivatives of thermodynamic properties with temperature, pressure, composition or other variables to be obtained. The tuning of an EoS model can be achieved by simulating the PVT studies using an EoS model, a stability algorithm, a flash algorithm and a saturation pressure algorithm. Then, the laboratory data are compared against the predictions of the EoS model; and then by tuning any uncertain parameters the minimization of their difference is achieved. In the current chapter, the stability and flash algorithm are described in detail. Figure 3.1 depicts the hierarchy of the tuning logic of an EoS. This chapter basically presents the stability algorithm, flash algorithm and the saturation pressure algorithm and how these algorithms are combined with an EoS model in order to simulate the CCE, DLE and ST experiments.

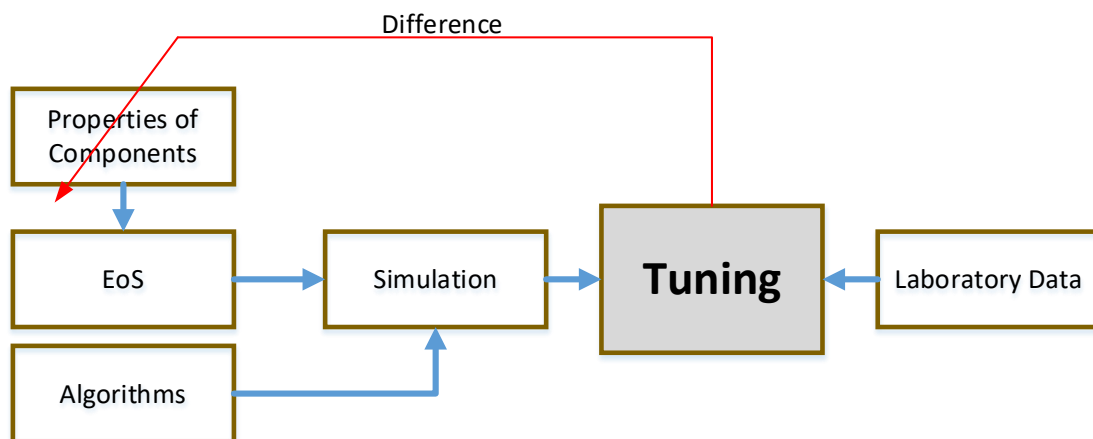


Figure 3.1: Tuning process of Equations of State.

3.1 Stability Analysis

The determination of phase stability, i.e., whether or not a given phase will split into multiple phases at certain pressure and temperature conditions, is a key step in vapor-liquid equilibrium (VLE) calculations and thus in the simulation of PVT studies. A phase is a chemically homogeneous, physically distinct and mechanically separable part of a system. The number of phases of a fluid mixture, at certain conditions, can be determined through stability analysis.

If the pressure is above the bubble point pressure, then the fluid exists in liquid state. However, when the pressure is above the upper dew point pressure or below the lower dew point pressure, the fluid exists in gas state. As might be expected, the fluid is a monophasic gas at any temperature above the cricondentherm and at any pressure. Since it is very costly to determine the saturation pressure and cricondentherm, Michelsen's approach is computationally preferable.

In 1982, Michelsen made use of numerical methods for deciding whether a phase is thermodynamically stable or not. In general, a thermodynamic system at a constant pressure and temperature has the tendency to minimize its Gibbs energy in order to reach the equilibrium state. Assuming that a homogeneous mixture (system) consisting of N_i moles exists, Michelsen suggested forming a second phase inside any given mixture to verify whether such a system is stable or not. The difference of Gibbs free energy between the split and the initial system is given by:

$$\Delta G = G^{\text{II}} - G^{\text{I}} \quad (3.1)$$

where,

G^{II} : Gibbs free energy of the system with an infinitesimal quantity of a second phase

G^{I} : initial system's Gibbs free energy

Michelsen proved that when the ΔG of the split and initial system is negative for at least one combination of infinitesimally small n_i moles, then there is at least one specific composition which when forming a second phase, the reduction of the total Gibbs free energy of the thermodynamic system takes place. Therefore, the thermodynamic system is eventually divided into two or more phases when arriving at thermodynamic equilibrium.

3.1.1 Michelsen's graphical solution of the stability test

Michelsen investigated phase stability analysis of multicomponent mixtures by means of the Gibbs Tangent Plane Distance (TPD) criterion. For a given temperature and pressure, the necessary and sufficient condition for a phase of composition \mathbf{z} to be stable is that the Gibbs free energy surface of the mixture is not intercepted by the tangent hyper plane at any composition \mathbf{x} . To fulfill this condition, the Gibbs tangent plane distance function, $TPD(\mathbf{x})$, must be nonnegative for any trial composition \mathbf{x} . Therefore, it is possible to examine whether a phase is stable by minimizing the $TPD(\mathbf{x})$ function, subject to mass balance constraints. If the tangent plane distance function at the global minimum point has a value greater than or equal to zero, then the analyzed phase is thermodynamically stable because the $TPD(\mathbf{x})$ function is also nonnegative for all compositions \mathbf{x} in the permissible region. If the $TPD(\mathbf{x})$ function is negative at its global minimum point, then the tangent plane lies above the Gibbs free energy surface, and hence the examined phase is unstable and will be split into new phases. Figure 3.2 describes schematically Michelsen's graphical solution of the stability test.

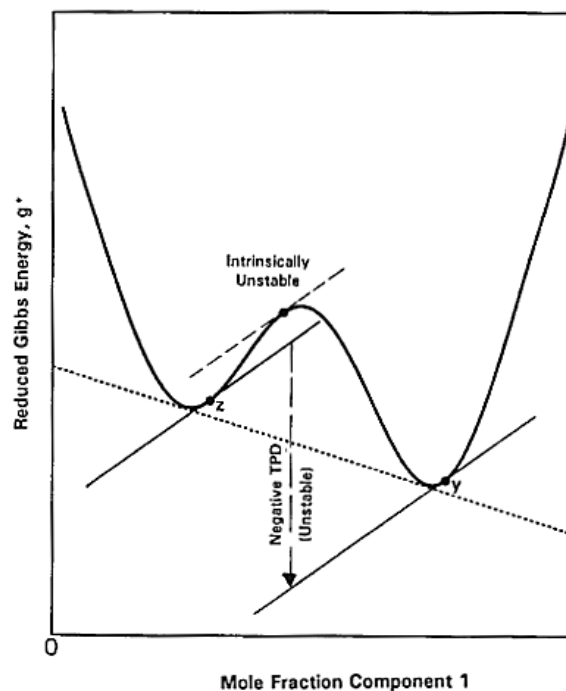


Figure 3.2: Michelsen's graphical solution of the stability test. (Whitson, 2000).

3.1.2 Michelsen's algorithm

The algorithm Michelsen devised to attach numerically phase stability is described below:

1) Calculate the mixture fugacity f using overall composition \mathbf{z} .

2) Estimate initial equilibrium ratios k_i using Wilson's correlation:

$$k_i = \frac{\exp[5.37(1+\omega_i)(1-T_{ri}^{-1})]}{P_{ri}}$$

3) It is assumed that initially the feed exists in liquid state and the composition of the bubble that will potentially decrease system's Gibbs energy is sought.

Calculate: $Y_i = k_i z_i$

4) Get the sum of the mole numbers: $S_V = \sum Y_i$

5) Normalize the second-phase mole numbers to get mole fractions $y_i = S_V / Y_i$ and calculate the second-phase fugacity f_i^y using the EoS model.

6) Calculate the corrections for k_i values: $R_i = \frac{1}{S_V} \cdot \frac{f_i^{(z)}}{f_i^{(y)}}$

7) Check if convergence is achieved: $\sum (R_i - 1)^2 < \varepsilon$

8) If convergence has not been attained, update the k_i values and return to step number 3: $k_i^{(n+1)} = k_i^{(n)} R_i^{(n)}$

9) A trivial solution is obtained if: $\sum (\ln k_i)^2 < \delta$

In the case in which the feed exists in gaseous phase, a liquid-like second phase is created. The previous steps are followed by replacing equations in steps 3, 4, 5 and 6 by equations (3.2), (3.3), (3.4) and (3.5) respectively.

$$X_i = z_i / k_i \tag{3.2}$$

$$S_L = \sum X_i \tag{3.3}$$

$$x_i = S_L / X_i \tag{3.4}$$

$$R_i = S_L \cdot \frac{f_i^{(z)}}{f_i^{(y)}} \tag{3.5}$$

Provided that the convergence of a solution yielding equilibrium phase compositions or a trivial solution is achieved, the interpretation of the results of this method is based on Table 3.1:

Table 3.1: Michelsen's algorithm results.

Vapor phase test	Liquid phase test	Result
Trivial solution	Trivial solution	Stable
$S_V \leq 1$	Trivial solution	Stable
Trivial solution	$S_L \leq 1$	Stable
$S_V \leq 1$	$S_L \leq 1$	Stable
$S_V > 1$	Trivial solution	Unstable
Trivial solution	$S_L > 1$	Unstable
$S_V > 1$	$S_L > 1$	Unstable
$S_V > 1$	$S_L \leq 1$	Unstable
$S_V \leq 1$	$S_L > 1$	Unstable

3.2 Flash Calculations

Before performing a flash calculation, the number of phases of the fluid mixture, which is being studied, must be known. This is the reason why a stability analysis, according to the algorithm Michelsen proposed, precedes. Once established that the feed will split into two or more phases, the flash calculation can be performed.

Flash calculations using EoSs are of major importance and an integral part of the calculations conducted in Petroleum Engineering. In principle, flash calculations are straightforward, they involve combining the VLE equations with the component mass balances and they are performed when the amount (moles) of the liquid and gas phase, coexisting in a reservoir, is required.

More specifically, if the composition \mathbf{z} of a hydrocarbon system is known, flash calculations at certain temperature and pressure conditions (Figure 3.3) will be run in order for the moles of the gas phase molar fraction (β), the liquid phase molar fraction

(1-β), as well as the composition of the equilibrating liquid \mathbf{x} and gas phase \mathbf{y} to be determined.

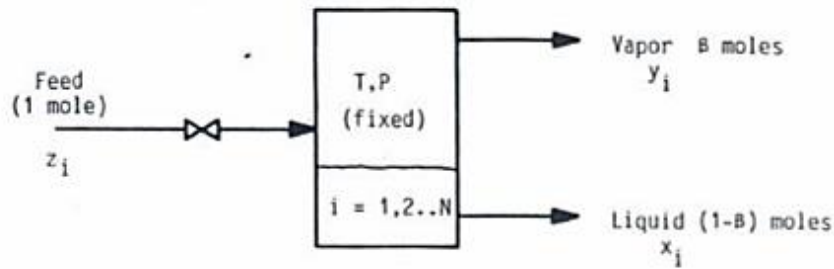


Figure 3.3: Schematic depiction of a flash cell (Pedersen, 1989).

3.2.1 Mathematical approach of flash problem

In order to solve a flash problem, two constraints must apply. These are the conservation of the mass and the equality of fugacities.

According to the mass balance, which essentially states that if the initial supply of \mathbf{z} , which consists of N moles, is divided into the gaseous phase (y_i) and the liquid phase (x_i), then the sum of the moles of the gas phase n_V and liquid phase n_L will be equal to N .

$$z_i N = y_i n_V + x_i n_L \quad (3.6)$$

According to the second constraint, i.e. the equality of fugacities, the Gibbs free energy of the final two-phase system must be minimum. Gibbs energy is expressed mathematically by the following expression:

$$G = (1 - \beta) \sum_{i=1}^n x_i \ln f_i^{(x)} + \beta \sum y_i \ln f_i^{(y)} \quad (3.7)$$

If the total free energy of the Gibbs system is at its minimum, then the fugacity of each component in the gaseous phase will be equal to the escape tendency of each component in the liquid phase: $f_i^L = f_i^V$

If the equality of fugacities of each component in the gas and in the liquid phase is further developed then the vapor-liquid equilibrium ratio is determined:

$$f_i^L = f_i^V \rightarrow \varphi_i^{(y)} y_i p - \varphi_i^{(x)} x_i p = 0 \rightarrow k_i = \frac{y_i}{x_i} = \frac{\varphi_i^{(x)}}{\varphi_i^{(y)}} \quad (3.8)$$

Finally, it must be ensured that the composition of each equilibrium phase sums up to unity.

$$\sum_{i=1}^n (x_i - y_i) = 0 \quad (3.9)$$

According to what mentioned, the flash problem is based on the solution of a system of $2N + 1$ equations, namely equations (3.8) and (3.9), in $2N + 1$ unknowns, i.e. y_i , x_i and β .

3.2.2 Solving the system of $2N+1$ equations and $2N+1$ unknowns

The solution of the system described in subsection 3.2.1 is quite complicated as the system consists of $2N + 1$ nonlinear equations and $2N + 1$ unknowns. However, if the k_i equilibrium ratios are introduced, then the system will automatically be converted to a system of $N + 1$ equations and $N + 1$ unknowns. Indeed, by introducing:

$$k_i = \frac{y_i}{x_i} \quad (3.10)$$

the liquid phase composition is obtained by:

$$x_i = \frac{z_i}{1 + \beta(k_i - 1)} \quad (3.11)$$

From equations (3.10) and (3.11), equation (3.12) arises:

$$y_i = \frac{z_i k_i}{1 + \beta(k_i - 1)} = k_i x_i \quad (3.12)$$

Substituting equations (3.11) and (3.12) into (3.9) gives the well-known Rachford-Rice equation which must be solved with respect to the β molar fraction, using the Newton-Raphson method. The liquid and gaseous phase compositions given in equations (3.11) and (3.12) are then determined and its equilibrium coefficients (3.10) are obtained. The process is repeated until the new k_i equilibrium ratio values converge and no longer change significantly.

3.3 Determination of saturation pressure

The bisection method, also known as the method of halving the interval, was used to find the saturation pressure. The first step in determining the saturation pressure was finding a random pressure over a closed interval at which the mixture sample is unstable. This pressure represented the lower bound (P_{lb}) of the search for the saturation pressure on the upper curve of the phase envelope. The upper bound (P_{ub}) of the closed interval represented the upper bound of the search. At this pressure (upper bound of the search), the mixture was stable.

The bisection method was given the initial interval $[P_{lb}, P_{ub}]$ that brackets the saturation pressure. At each iteration, the numerical method cut the interval into two halves and it was checked which half interval contained the saturation pressure using the stability algorithm. The search by halving the interval while keeping enclosed the saturation pressure continued until the search interval was satisfactory small $|P_{ub} - P_{lb}| < \text{tol}$. In any case, an exact solution was not found, rather a numerical solution that is acceptably close to the true solution.

3.4 Simulation of PVT Experiments

The simulation of the CCE test utilizing an EoS model consists of a series of combinations of stability analyses and calculations. As far as the DLE test and the ST are concerned, the simulation of these tests does not require a stability analysis as on the one hand they consist of a series of flashes at pressures below the saturation pressure point and on the other hand at each pressure step the composition of the feed is equal to the composition of the liquid phase at the previous step.

3.4.1 Simulation of the Constant Composition Expansion test

For each pressure P_i , which may be above or below the saturation point pressure, at which the CCE test is conducted:

Step 1: A stability test takes place. If the fluid exists in one phase, then the molar volume occupied by $N_F = 1$ mol of the hydrocarbon system is calculated using the EoS:

$$V_{m,\text{tot}}(P_i) = \frac{N_F Z R T_{\text{res}}}{P_i} \quad (3.13)$$

Step 2: If a two-phase equilibrium is established, then a flash calculation of the feed composition, \mathbf{z} , is performed at current pressure and temperature step of CCE. As a result, the values of x_i , y_i , β , Z^l , Z^v , are obtained. The volumes of the liquid and gas phase can be estimated using the following expressions:

$$V_l(P_i) = \frac{N_F(1-\beta)(P_i)Z^l(P_i)RT_{\text{res}}}{P_i} \quad (3.14)$$

$$V_v(P_i) = \frac{N_F\beta(P_i)Z^v(P_i)RT_{\text{res}}}{P_i} \quad (3.15)$$

$$V_{\text{tot}}(P_i) = V_l(P_i) + V_v(P_i) \quad (3.16)$$

Step 3: The saturation pressure point (P_{sat}) using an independent algorithm as well as the volume at the saturation point V_{sat} are computed.

After completing the aforementioned calculations, the determination of the following properties takes place:

1) Calculate the relative volume from the following expression:

$$V_r(P_i) = \frac{V_{\text{tot}}(P_i)}{V_{\text{sat}}} \quad (3.17)$$

2) Calculate the isothermal compressibility at each pressure step above the saturation point pressure by numerically differentiating the relative volume:

$$c(P_i) \approx - \frac{1}{\frac{V_{\text{tot}}(P_i) + V_{\text{tot}}(P_{i+1})}{2}} \frac{V_{\text{tot}}(P_i) - V_{\text{tot}}(P_{i+1})}{P_i - P_{i+1}} \quad (3.18)$$

The flow diagram of the simulation of the CCE test using an EoS is given in Figure 3.4.

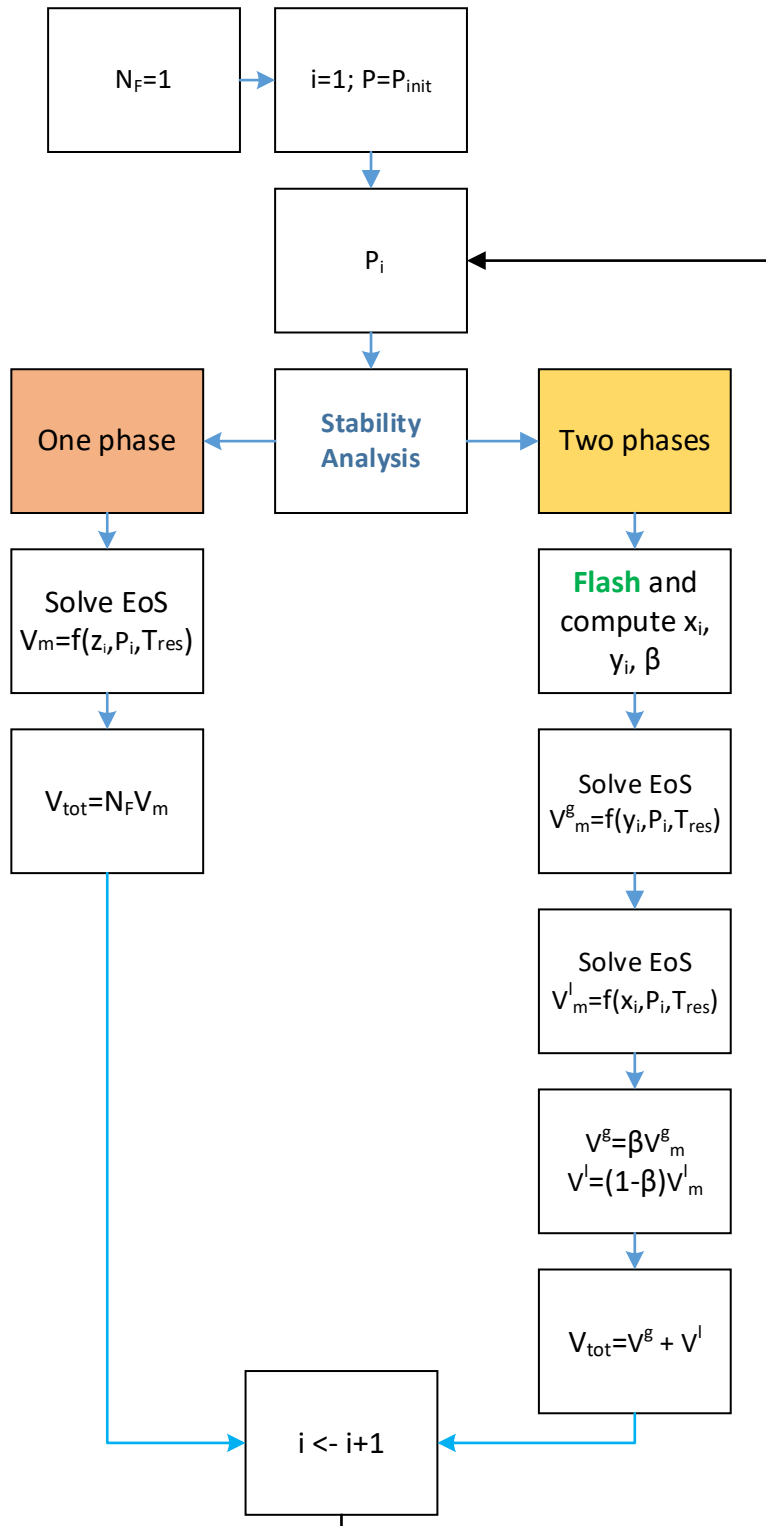


Figure 3.4: Flow diagram of the simulation of the Constant Composition Expansion test.

3.4.2 Simulation of the Differential Liberation Expansion test

Step 1: Starting with the saturation point pressure, P_{sat} , and reservoir temperature, T_{res} , calculate the volume occupied by $N_F = 1$ mole of the hydrocarbon system with an overall composition of \mathbf{z} :

$$V_{\text{sat}} = \frac{N_F Z_{\text{sat}} R T_{\text{res}}}{P_{\text{sat}}} \quad (3.19)$$

Step 2: Reduce the pressure to a predetermined value of P at which the equilibrium ratios are calculated and used to perform flash calculations. The actual number of moles of the liquid phase ($1-\beta$), with a composition of x_i , and the actual number of moles of the gas phase (β), with a composition of y_i are determined. The molar volumes of each phase are computed as follows:

$$V_l(P_i) = \frac{(1)(1-\beta)Z^l R T_{\text{res}}}{P_i} \quad (3.20)$$

$$V_v(P_i) = \frac{(1)\beta Z^v R T_{\text{res}}}{P_i} \quad (3.21)$$

The volume of the liberated solution gas as measured at standard conditions is determined from the following expression:

$$G_p = 379.4\beta, \text{ in ft}^3/\text{lb mol} \quad (3.22)$$

The total cumulative gas produced at any depletion pressure, P , is the cumulative gas liberated from the crude oil sample during the pressure reduction process (sum of all the liberated gas from previous pressures and current pressure) as calculated from the expression:

$$G_{P,\text{cumulative}} = \sum_{P_{\text{sat}}}^P G_p \quad (3.23)$$

Step 3: All the equilibrium gas at each pressure step P_i , is removed and the total composition of the subsequent step equals to x_i , which is the composition of the liquid phase in the next step.

$$z_i(P_{i+1}) = x_i(P_i) \quad (3.24)$$

$$N_F(P_{i+1}) = N_F(P_i) (1 - \beta)(P_i) \quad (3.25)$$

Step 4: Using the new overall composition and total moles, steps 2 through 3 are repeated. When the depletion pressure reaches the atmospheric pressure, the

temperature changes to 60°F and the residual-oil volume (V_{residual}) is calculated. The total volume of the gas evolved from the oil and produced is the sum of all-liberated gases including that at atmospheric pressure (G_{Total}).

Step 5: The calculated volumes of the oil and removed gas then are divided by the residual- oil volume to calculate the relative-oil volumes (B_o) and the solution R_s at all selected pressure levels from:

$$B_o(P_i) = \frac{V_i(P_i)}{V_{\text{residual}}} \quad (3.26)$$

$$R_s(P_i) = \frac{G_{\text{Total}} - G_{P,\text{cumulative}}}{V_{\text{residual}}} \quad (3.27)$$

The flow diagram of the simulation of the DLE test using an EoS is presented in Figure 3.5.

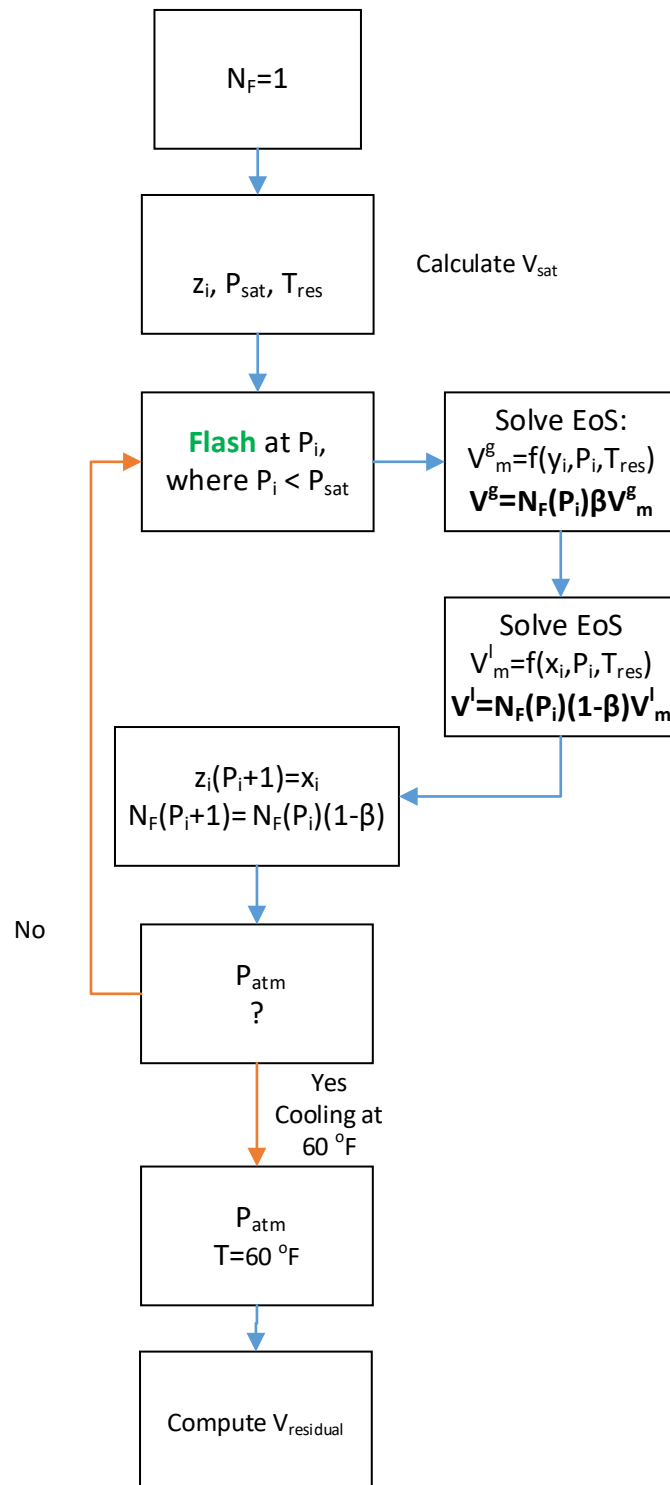


Figure 3.5: Flow diagram of the simulation of the Differential Liberation Expansion test.

3.4.3 Simulation of the Separator Test

The ST simulation is similar to the DLE test simulation. Practically, the ST is a variation of the DLE experiment where the pressure from the saturation point pressure is gradually reduced to 14.7 psia, while the temperature is reduced from the reservoir temperature to 60°F.

The flow diagram of the simulation of the ST using an EoS is presented in Figure 3.6.

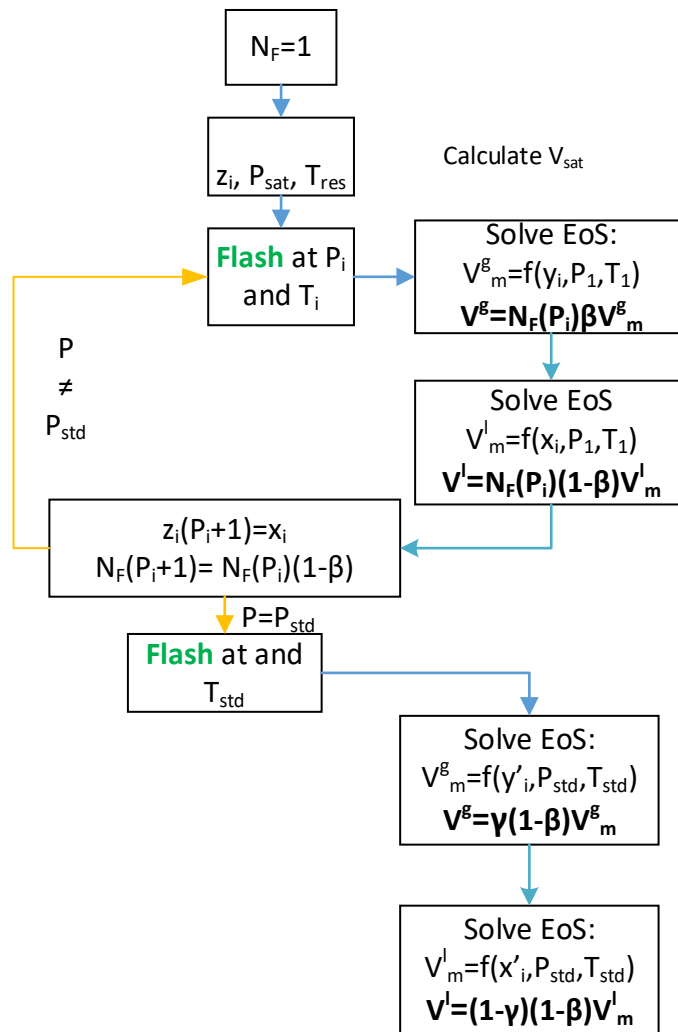


Figure 3.6: Flow diagram of the simulation of the Separator Test.

4. Cubic Equations of State

As mentioned in Chapter 1 of this Master Thesis, Equations of State (EoSs) are mathematical expressions that relate pressure (P), volume (V), temperature (T) and composition (z) of a reservoir fluid system. These equations are called Equations of State because they describe the state of a fluid at specific conditions of pressure and temperature.

Without any doubt, the development of the Equations of State can be deemed as quite impressive. The first EoS that has ever been developed is the Ideal Gas Law. This was developed by combining Boyle's, Charle's and Gay-Lussac's law. However, van der Waals was the one that made the real breakthrough in the field of EoSs by introducing the first cubic Equation of State (van der Waals cubic Equation of State, vdW cEoS) for the description of the thermodynamic behavior of a single-component fluid.

The Soave-Redlich-Kwong (SRK) and Peng-Robinson (PR) Equations of State are the cubic EoSs that are widely used in the modern oil and gas industry. These equations are used extensively for oil and gas reservoir modeling with a compositional simulator as long as they have been tuned against experimental data that have been generated in the PVT laboratory at specific pressures and temperatures.

The current chapter presents the Peng- Robinson cubic Equation of State as well as the requirements that the PR cEoS must fulfill in order to be used as a computational tool in the simulation of the PVT studies.

4.1 Peng-Robinson cubic Equation of State (PR EoS)

In 1976, Peng and Robinson introduced a variation of the van der Waals cubic Equation of State that improved the liquid density prediction. In terms of the molar volume (V_m), Peng and Robinson proposed the following two-constant cubic EoS:

$$P = \frac{RT}{V_m - b} - \frac{\alpha\alpha(T)}{V_m(V_m + b) + b(V_m - b)} \quad (4.1)$$

where,

$$\alpha(T) = [1 + m(1 - \sqrt{T_r})]^2 \quad (4.2)$$

$$m = \begin{cases} 0.37464 + 1.54226\omega - 0.2699\omega^2 & \omega \leq 0.49 \\ 0.3796 + 1.485\omega - 0.1644\omega^2 + 0.01667\omega^3 & \omega > 0.49 \end{cases} \quad (4.3)$$

$$\alpha_c = 0.45724 \frac{R^2 T_c^2}{P_c} \quad (4.4)$$

$$b_c = 0.07780 \frac{RT_c}{P_c} \quad (4.5)$$

In cubic form, PR cEoS is represented as:

$$V_m^3 - \left(b + \frac{RT}{P}\right) V_m^2 + \left(3b^2 + 2b \frac{RT}{P} - \frac{\alpha}{P}\right) V - \left(b^3 + b^2 \frac{RT}{P} - b \frac{\alpha}{P}\right) = 0 \quad (4.6)$$

or equivalently in a dimensionless form as:

$$Z^3 - (1 - B)Z^2 + (A - 3B^2 - 2B)Z - (AB - B^2 - B^3) = 0 \quad (4.7)$$

where,

$$A = \frac{\alpha \alpha(T) P}{(RT)^2} \quad (4.8)$$

$$B = \frac{bP}{RT} \quad (4.9)$$

4.2 Critical properties and acentric factor

The calculations performed using the cubic Equations of State for the estimation of the molar volume of the pure component at specific pressure and temperature conditions require, as depicted in figure 4.1, the determination of the properties of the critical temperature (T_c), the critical pressure (P_c) and the acentric factor (ω), for each component of the mixture. The critical properties and the acentric factor are used in order for the parameters α , b and m of the Peng-Robinson cubic Equation of State to be computed. Katz table provides the critical properties of pure and of pseudo- components in a mixture.

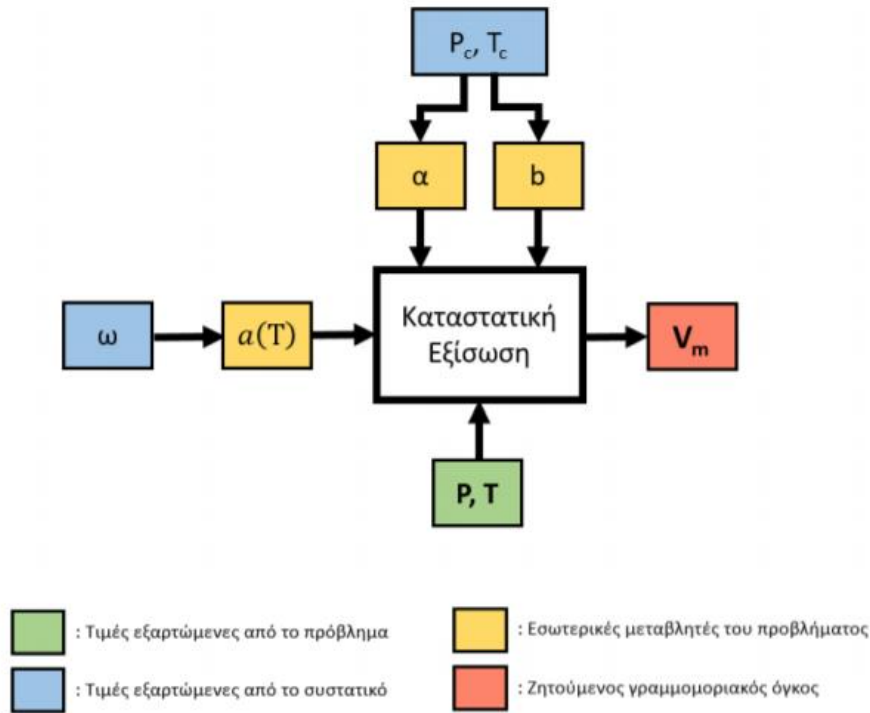


Figure 4.1: Estimation path of the molar volume of pure components.

The critical properties of the heavy fraction must be determined from correlations. Sutton reported that the Kessler-Lee equations provide the lowest error in comparison with other methods. Given specific gravity (SG) and boiling point (T_b) of the heavy fraction, physical properties are estimated as follows:

- **Critical Temperature**

$$T_c = 1.8 \left[189.8 + 450.6SG + (0.4244 + 0.1174SG)k + \frac{(0.1441 - 1.0069SG)10^5}{k} \right] \quad (4.10)$$

where,

$$k = T_b / 1.8 \quad (4.11)$$

- **Critical Pressure**

$$P_c = 14.5038 \exp \left\{ 5.689 - \frac{0.0566}{SG} - \left(0.43639 + \frac{4.1216}{SG} + \frac{0.21343}{SG^2} \right) \frac{k}{10^3} + \left(0.47579 + \frac{1.182}{SG} + \frac{0.15302}{SG^2} \right) \frac{k^2}{10^6} - \left(2.4505 + \frac{9.9099}{SG^2} \right) \frac{k^3}{10^{10}} \right\} \quad (4.12)$$

- **Acentric factor**

ω

$$= \begin{cases} -7.904 + 0.1352K - 0.007465K^2 + 8.359T_{br} + \frac{(1.408 - 0.01063K)}{T_{br}}, & T_{br} > 0.8 \\ \frac{-\ln\left(\frac{P_c}{14.696}\right) - 5.92714 + \frac{6.09648}{T_{br}} + 1.28862 \ln(T_{br}) - 0.169347T_{br}^6}{15.2518 - \frac{15.6875}{T_{br}} - 13.4721 \ln(T_{br}) + 0.43577T_{br}^6}, & T_{br} \leq 0.8 \end{cases} \quad (4.13)$$

where,

$$T_{br} = \frac{T_b}{T_c} \quad (4.14)$$

$$K = \frac{T_b^{1/3}}{SG} \quad (4.15)$$

4.3 Mixing rules and binary interaction coefficients

The Peng-Robinson cubic Equation of State requires the use of mixing rules for the description of the thermodynamic behavior of mixtures.

The attraction parameter $[\alpha\alpha(T)]_m$ and the repulsion parameter b_m in the Peng-Robinson Equation of State are determined for a given mixture by:

$$[\alpha\alpha(T)]_m = \sum_{i=1}^c \sum_{j=1}^c z_i z_j (1 - k_{ij}) \sqrt{\alpha_i \alpha_j \alpha_i \alpha_j} \quad (4.16)$$

$$b_m = \sum_{i=1}^c z_i b_i \quad (4.17)$$

where,

z: the composition of the mixture

c: number of pure components and

In the expression (4.16), k_{ij} is called binary interaction coefficient (BIP), where $k_{ii} = 0$ and $k_{ij} = k_{ji}$. BIPs vary depending on the Equation of State, the type of components and the possibly on the prevailing conditions.

4.4 Volume shift

Liquid volume predictions have never been accurate with two-parameter cubic EoSs such as the Peng-Robinson one. A comparison between the predicted liquid molar volume and the experimental data of pure compounds generally shows a systematic deviation. This volume translation or volume shift parameter technique can compensate

the weakness in molar liquid volumetric predictions by two-constant EoS. Jhaveri and Youngren (1988) firstly applied the volume shift technique to the PR EoS. Volume shift is applied to the calculated molar volume by EoS in the following form:

$$V_{\text{corr}}^L = V_L - \sum(x_i \cdot c_i) \quad (4.18)$$

where,

V_{corr}^L : the corrected molar volume

V_L : the molar volume by EoS

x_i : the mole fraction of component i

c_i : the volume shift parameter for component i

4.5 Lumping and delumping method

A proper description of the heavy hydrocarbon fractions cannot be accomplished by simply using the correlations mentioned in subchapter 4.2 to estimate the physical properties of the heavy fraction. In order to get accurate estimations using an EoS, it is necessary a lumping and delumping method to be used to estimate the properties or behavior of liquid and/or vapor hydrocarbon phases from data relative to a reference set of hydrocarbon mixtures in a series of thermodynamic states in a medium.

First, the heavy fraction is split into an arbitrary number of discrete pseudocomponents. In this Master Thesis, the molar distributions were described by the continuous gamma distribution model. More specifically, this model is based on the three-parameter gamma probability density function:

$$p(M) = \frac{(M-\eta)^{\alpha-1} \exp[-\frac{M-\eta}{\beta}]}{\beta^\alpha \Gamma(\alpha)} \quad (4.19)$$

where:

$$\beta = (M_{n+} - \eta) / \alpha \quad (4.20)$$

α : the parameter that controls the shape of the distribution

η : the lowest molecular weight in the distribution

M : the molecular weight that is defined as the variable for molar distribution described by parameters η , α and β .

With extended Gas Chromatography data available on most samples in a field or basin, the field-wide gamma model generally has a common shape (α), lower MW bounds (M_{Li}), where $\eta = M_{Ln}$, and sample-specific average MWs (M_{n+}).

The pseudocomponents should be later lumped into a smaller number of pseudocomponents. In the subsequent stage, the Lee-Kessler correlations are used to estimate the critical properties and the acentric factor of the lumped pseudocomponents.

It should be mentioned that the lumping and delumping scheme described above was performed by the operator and is not a part of this Master Thesis' developed tuning algorithm.

5. Tuning Methodology

The tuning of an EoS model follows after the characterization of the heavy fraction. More specifically, the tuning of an EoS is the process of adjusting its tunable parameters in order to achieve a satisfactory match between the laboratory fluid PVT data and the data resulting from the Equation of State used. In order for an EoS to be properly adjusted to a multicomponent system, it is essential to take into consideration its intrinsic limitations as well as to perform a proper characterization of the components of the hydrocarbon mixtures, due to the inaccuracy of the critical components of the heavy fraction and the lumped components. In addition, it is essential to determine the binary interaction coefficients (BIPs), k_{ij} , that account for the possible interactions in each couple of components of a multicomponent system and are used in the calculation of the parameter of attraction. Following the above procedure, a number of parameters of the EoS can be adjusted (tuning of EoS parameters), i.e. find suitable parameter values that lead to the optimization of the match between the available experimental data and the EoS predicted thermodynamic behavior of a multicomponent hydrocarbon mixture. This process is complicated while at the same time requires careful inspection of the physical interpretation of the values assigned to each tuned parameter. Simply put, it is of significant importance to pay particular attention to the physical soundness of the values attributed to the regression parameters apart from attempting to minimize the global error. Some of the physical constraints implemented for the tuning of the PR EoS in this Master Thesis impose the hierarchy of the components' properties, the computed curvature of the phase envelopes and the distribution of the partial derivatives of the volumetric properties with respect to the fluids' composition.

Laboratory data obtained from experimental pressure-volume-temperature (PVT) studies are used to adjust the EoS models. The most common used data are:

- Saturation point pressure: the bubble point pressure (P_b) for oils or the dew point pressure (P_d) for gas condensates.
- Data resulting from conducting the Constant Composition Expansion (CCE) experiment.
- Data resulting from conducting the Differential Liberation Expansion (DLE) experiment.
- Data resulting from conducting the Separator Test (ST).

In a cubic Equation of State model there are several parameters that can be adjusted. The most common parameters selected are referred below:

- The critical properties T_c , P_c of the non-well defined components.
- The acentric factor ω of the non-well defined components.
- The binary interaction coefficients, k_{ij} . When there are significant differences in the size and type of mixture molecules, especially in methane-containing mixtures, the binary interaction coefficients are of great importance. They are also necessary in the presence of non-hydrocarbons in a mixture, such as CO_2 , H_2S , N_2 , etc. Usually, these coefficients are derived directly from experimental equilibrium data of binary systems. However, they are not available for any kind of mixture that may be of interest. The usual factors that are usually considered are:
 - The binary interaction coefficients k_{ij} between CH_4 and the heavy fraction (fraction C_{n+}).
 - The binary interaction coefficients k_{ij} between CH_4 and non-hydrocarbon components, such as N_2 , CO_2 and H_2S , when their content in petroleum fluid is significant.
 - The binary interaction coefficients k_{ij} between the heavy fraction and non-hydrocarbon components, such as N_2 , CO_2 and H_2S , when their content in the petroleum fluid is significant.

6. Optimization

The EoS tuning procedure against a set of laboratory data is basically an optimization problem during which the minimization of the global error is attempted by adjusting the values of selected regression parameters. This chapter serves as an introduction to the pattern search method and presents the tuning of an EoS model as an engineering optimization problem.

6.1 What is optimization?

Optimization can be defined as the act of obtaining the best result under given circumstances. In practice, engineers need to take many technological decisions at several stages. The ultimate goal of all such decisions is either to minimize the effort and cost required or to maximize the desired benefit. Since the effort required or the benefit desired in any practical situation can be expressed as a function of certain decision variables, optimization can be described as the process of finding those variables' values that result to the maximum or minimum value of a function. If a point x^* (Figure 6.1) corresponds to the value that minimizes function $f(x)$, the same point also corresponds to the value that maximizes the negative of the function, $-f(x)$. Thus without loss of generality, optimization can be taken to mean minimization since the maximum of a function can be found by seeking the minimum of its negative.

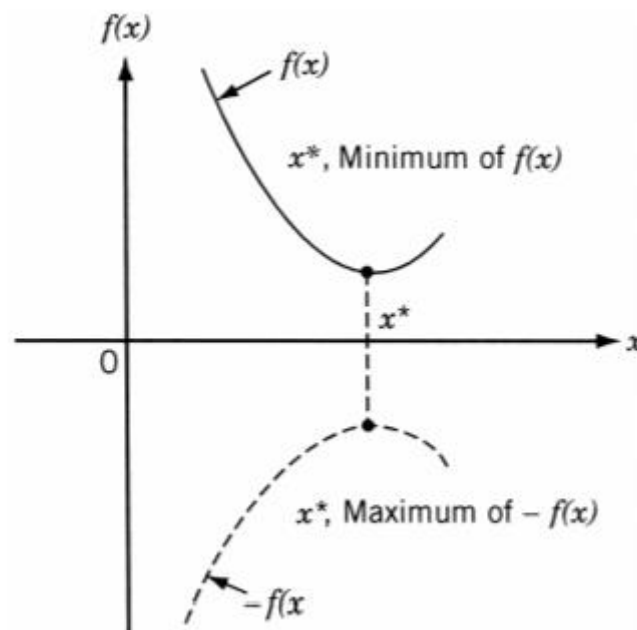


Figure 6.1: Minimum of $f(x)$ is same as maximum of $-f(x)$.

The mathematical function that is to be optimized is known as the objective function, usually containing several variables. An objective function can be a function of a single variable for some practical problems; however, a single variable function may not be challenging from an optimization point of view. Optimization problems may involve more than one objective function and are known as multi-objective optimization problems. Depending on the nature of the problem, the variables in the model may be real or integer (pure integer or binary integer) or a mix of both. The optimization problem could be either constrained or unconstrained.

It is important to elucidate that optimization solvers have their disadvantages, the most important of which is getting stuck at a local minimum, which is an issue that concerns non-convex problems (the majority of engineering problems are non-convex). Therefore, there is no single method for efficiently tackling all optimization problems. As a result, a number of optimization methods have been developed. In this Master Thesis, the pattern search method was selected for tuning the PR EoS model because it guarantees convergence to global minimum.

6.2 Pattern search method

Pattern search (also known as direct search, derivative-free search, or black-box search) is a family of numerical optimization methods that does not require a gradient. As a result, it can be used on functions that are not continuous or differentiable.

Pattern search methods follow the general form of most optimization methods in that they are provided by the user with an initial guess of the solution x_0 and an initial choice of a step length parameter $\Delta_0 > 0$. Pattern search methods are characterized by a series of exploratory moves that investigate the performance of the objective function. This performance is evaluated at a pattern of points, all lying on a rational lattice around the current solution estimate. The exploratory moves consist on a systematic strategy of visiting the points in the lattice, in the instant neighborhood of the current iterate. If an exploratory move leads to a decrease in the value of f it is called a success (Figure 6.2); otherwise it is called a failure (Figure 6.3).

The pattern search algorithm keeps track of the direction of travel as the process moves from point to point. The first step is providing a initial point, x_0 , at which the pattern search method begins. In Figure 6.2, the coordinates of the initial point x_0 are (2.1,1.7). At this point, the value of the objective function is 4.6347. At the first iteration, the

mesh size is 1 and the pattern search algorithm proceeds by conducting exploratory moves in all directions (East, North, West and South). In the subsequent stage, the algorithm polls the mesh points by computing their objective function values until it finds one whose value is smaller than 4.6347. In this case, the first such point it finds is (1.1, 1.7). At this point, the value of the objective function is 4.5146, so the poll at iteration 1 is successful. The algorithm sets the next point in the sequence equal to $x_1 = (1.1, 1.7)$ and repeats the aforementioned procedure by multiplying the current mesh size by 2. If the poll is unsuccessful in a subsequent iteration, i.e. Figure 6.3, the function value at this iteration remains unchanged from the previous iteration. By default, the pattern search doubles the mesh size after each successful poll and halves it after each unsuccessful poll. Increasing the mesh size allows the algorithm to avoid local minima. The algorithm stops when the mesh size is less than the tolerance value.

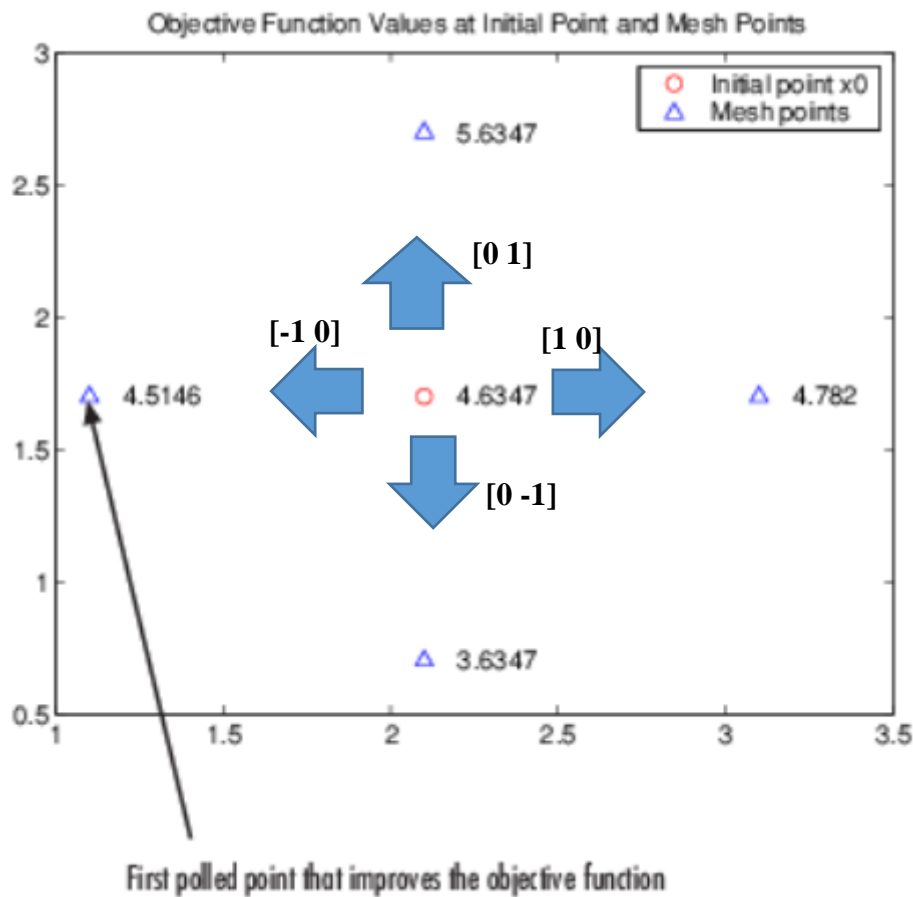


Figure 6.2: Example of successful poll (www.mathworks.com).

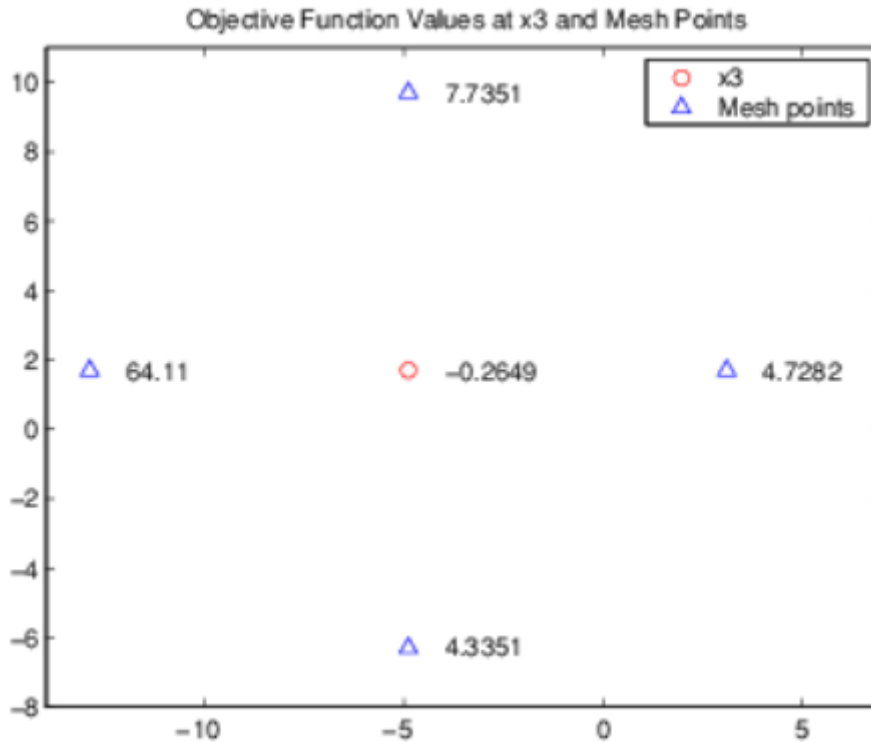


Figure 6.3: Example of unsuccessful poll (www.mathworks.com).

6.3 Development of the objective function and pattern search implementation for EoS tuning

An integral part of the tuning of an EoS model consists of defining the objective function. In this Master Thesis, the objective function was defined as the sum of the sums of squares of weighted errors between the measured lab PVT data per PVT experiment (i.e. CCE, DLE and ST experiments) and corresponding EoS estimations. The weights, which are associated with each PVT data item or group of PVT data, is a user-assigned weighting factor and is used to assign a degree of importance to each data point. Then, the pattern search method was implemented in order to minimize the aforementioned nonlinear objective function by adjusting a set of tunable parameters selected by the user. The bounds of the optimization problem were imposed by the box constraints of the developed software. At this point, it is of critical importance to highlight that the available tunable parameters of the developed algorithm are the critical pressure, critical temperature, molecular weight, volume shift parameter and the binary interaction coefficients of the components of the petroleum mixture being studied.

7. Results

7.1 Four-component synthetic mixture

The optimizer's efficiency was first evaluated using a simple four-component synthetic mixture, the composition of which is depicted in Table 7.1. The four-component synthetic mixture optimization problem is constrained, which simply means that the choice variables are allowed to get only in predefined range.

Table 7.1: Composition of the four-component synthetic mixture.

Component	Composition (%)
C ₁	30
n - C ₅	15
C ₁₀	30
C ₂₀	25

Firstly, the CCE and DLE experiments were simulated by the WinProp simulator using the four-component synthetic mixture. Next, the same experiments were simulated using the CCE and DLE simulators developed in Matlab. When comparing the estimations of WinProp and Matlab simulator, it was confirmed that the two simulators produce the same results if and only if the component properties share exactly the same values. Subsequently, six different tuning scenarios were developed, in each one of which initial values, different from the real ones, implemented in WinProp ones, were assigned to selected component parameters. In each case, the efficiency of the optimizer to drive the parameter values, as close as possible to the real ones after the tuning process was tested. The weight factors used during optimization were set equal to unity for all properties, except for the weight factor corresponding to compressibility, which was set equal to zero. This strategy was simply followed because of the fact that the way isothermal oil compressibility above the bubble point is computed in the WinProp simulator is slightly different than the one used in the Matlab CCE simulator, thus resulting to an error of approximately 0.5%, even when all the component properties are assigned a standard error, WinProp derived methods.

7.1.1 First Case Scenario – Synthetic mixture

In the first case scenario, the critical pressure of the fourth component of the synthetic mixture was chosen to be the tunable parameter. A random number generator between 1.2 and 1.6 MPa provided the initial guess for the optimization algorithm. The real value of the critical pressure of the fourth component is equal to 1.455 MPa as derived from WinProp software. Table 7.2 shows the optimized value obtained by the optimizer, which was developed in Matlab, after the tuning process and it can be seen that it is very close to the real one.

Table 7.2: Optimized value of P_c (MPa) in the first case scenario.

Type	Number	Exact Value	min	max	Optimized Value
P_c	4	1.455	1.200	1.600	1.455

Figure 7.1 confirms that the point at which the objective function exhibits a global minimum, the smallest overall value of the objective function, is about 1.45×10^6 Pa; in other words, when the P_c of the fourth component equals to the nominal one.

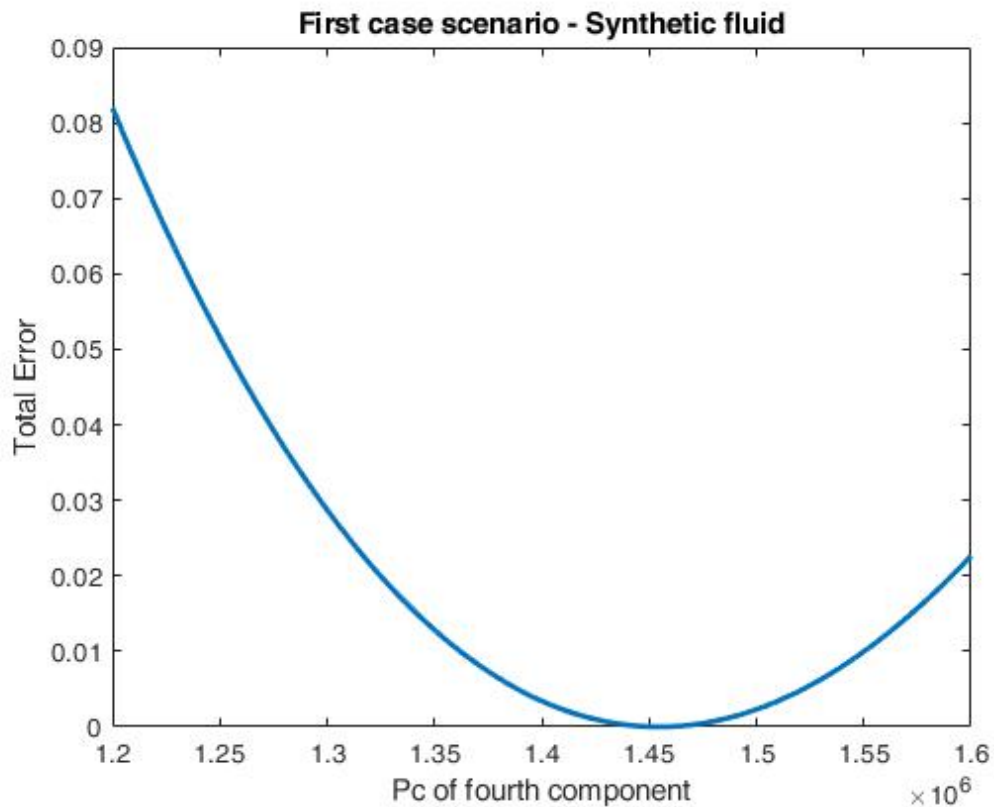


Figure 7.1: Total Error vs P_c of 4th component – Synthetic mixture.

7.1.2 Second Case Scenario – Synthetic mixture

In the second case scenario, the binary interaction coefficient of C_1 and C_{20} of the synthetic mixture was chosen to be the tunable parameter. A random number generator between -0.05 and 0.2 provided the starting point for the optimization algorithm. At this point, it should be highlighted that the exact value of the binary interaction coefficient of CH_4 and C_{20} was set equal to zero. Table 7.3 depicts the optimized value obtained by the optimizer after the tuning process and it can be observed that it is very close to zero.

Table 7.3: Optimized value of BIC in the second case scenario.

Type	Components	Exact Value	min	max	Optimized Value
k_{ij}	C_1 and C_{20}	0.00	-0.05	0.20	0.0015

Figure 7.2 confirms that the global minimum of the objective function is attained when the binary interaction coefficient of C_1 and C_{20} of the synthetic mixture is set to zero. The BIC is allowed to be as low as -0.2 for visualization purposes.

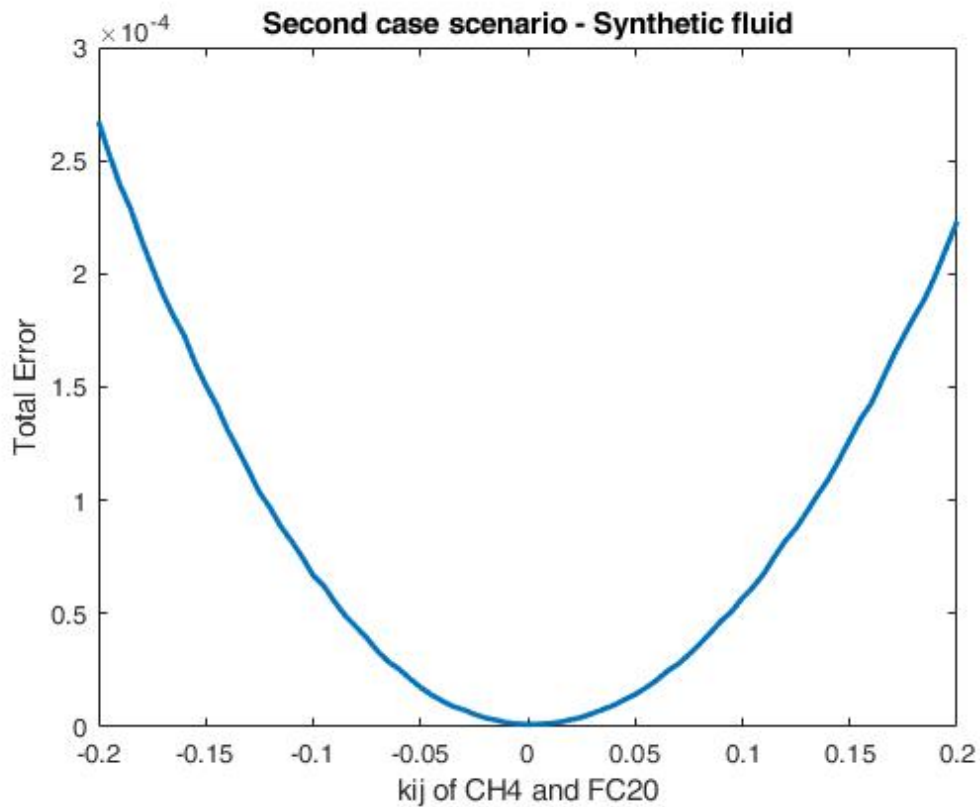


Figure 7.2: Total Error vs k_{ij} of CH_4 and C_{20} – Synthetic mixture.

An interesting point worth mentioning is the fact that the graph of the objective function (Figure 7.2), is not symmetrical about the Total Error axis. This is to be expected as the effect on the total error will not be the same if the value of the k_{ij} is increased or if the value of the k_{ij} is decreased by the same quantity.

7.1.3 Third Case Scenario – Synthetic mixture

In the third case scenario, the critical temperatures of the third and fourth component of the synthetic mixture were selected to be the tunable parameters. A random number generator provided initial guesses for the optimization algorithm. The real values of the critical temperature of the third and fourth component are 622.1 and 782.9 K respectively. Table 7.4 depicts the optimized values obtained after the tuning process and it can be observed that the optimized values match the real ones.

Table 7.4: Optimized value of the T_c of third and fourth component in the third case scenario.

Type	Number	Exact Value	min	max	Optimized Value
T_c	3	622.10	450.00	700.00	622.02
	4	782.90	520.00	900.00	783.14

The objective function contour plots in Figure 7.3 are useful for visualizing the functional space of the 2D optimization problem of the third tuning scenario. The red circle point represents the exact values of the critical temperatures of the third and fourth component, whereas the two black lines represent the major and minor axis of the ellipse. It can be seen that the red circle point is placed inside of the dark-blue contour error and it is the center of the ellipse. In other words, it is the global minimum of the objective function, which is a strictly convex function. Another important observation is the fact that the objective function is not sensitive along the major axis direction, which renders the minor axis direction a more preferable direction for the optimizer to move along. However, since the optimizer used in this Master Thesis is not a gradient-based optimizer, we cannot expect that the optimizer will be able to distinguish the difference in the sensitivity of the objective function along the two axes and eventually move parallel to the minor axis if needed, to arrive to the red point.

The conclusion derived from the third case scenario is that if during the optimization one component becomes heavier (T_c is increased) and the other component lighter

(T_c is decreased), the effect on the objective function will not be as great as it would be in the case that both components would become either heavier or lighter.

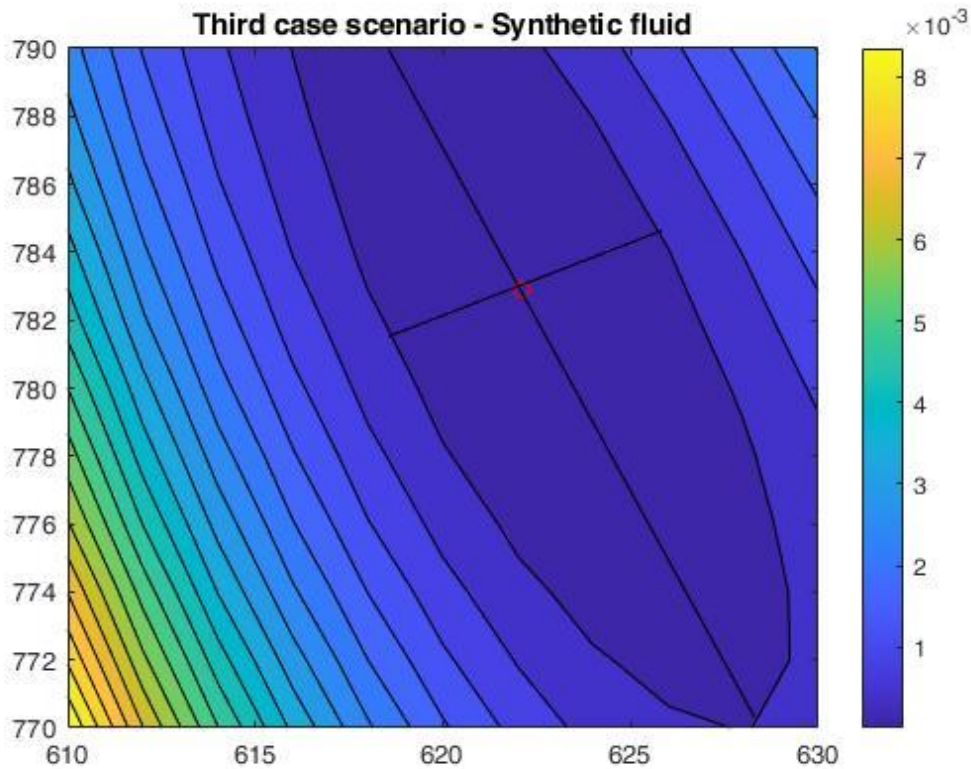


Figure 7.3: Contour plot of the 2D optimization problem of the third case scenario.

7.1.4 Fourth Case Scenario – Synthetic mixture

In the fourth case scenario, the acentric factors (ω) of the third and fourth component of the synthetic mixture were chosen to be the tunable parameters. A random number generator provided the starting points for the optimization algorithm. The real values of the omega of the third and fourth component are 0.443774 and 0.816053 respectively. Table 7.5 shows the optimized values obtained after the tuning process and it can be observed that they are very close to the real ones.

Table 7.5: Optimized value of ω of third and fourth component in the second case scenario.

Type	Number	Exact Value	min	max	Optimized Value
Omega	3	0.444	0.355	0.532	0.443
	4	0.816	0.653	0.979	0.816

The red circle point in Figure 7.4 represents the exact values of the acentric factors of the third and fourth component, whereas the two black lines represent the major and

minor axes of the ellipse. It can be seen that the red circle point is placed inside the dark-blue contour and it is the center of the ellipse that is the minimum of the objective function. The interpretation of the fourth case scenario is similar to the interpretation of the third one. Therefore, the conclusion that can be derived from the fourth scenario is similar to that of the third one.

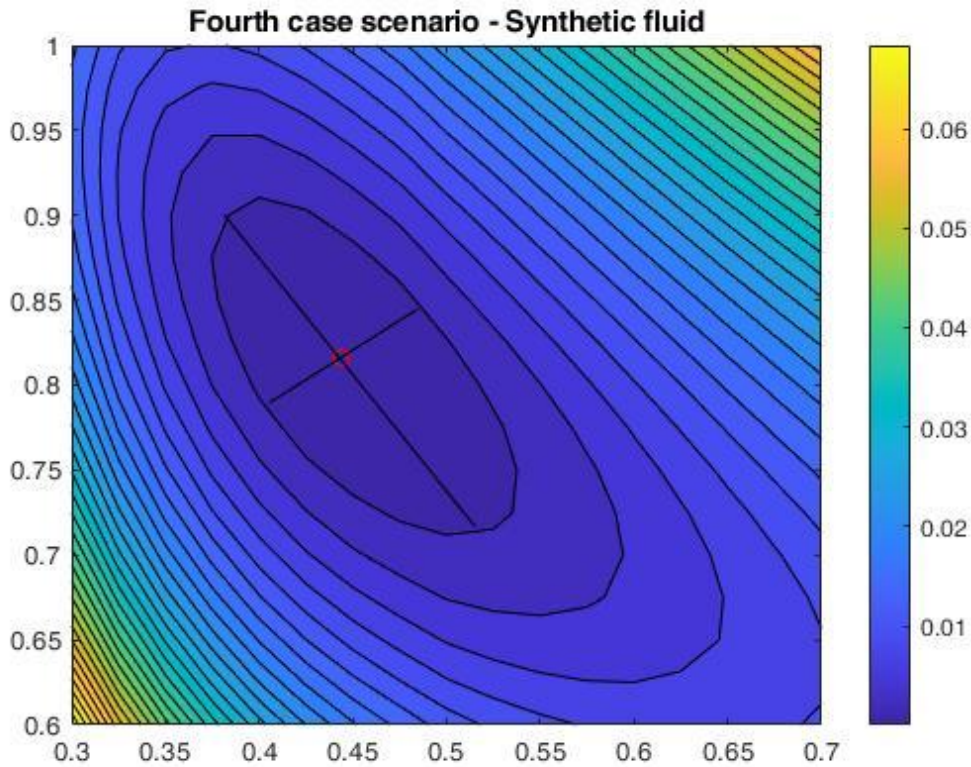


Figure 7.4: Contour plot of the 2D optimization problem of the fourth case scenario.

7.1.5 Fifth Case Scenario – Synthetic mixture

In the fifth case scenario, the critical temperatures of the second, third and fourth component of the synthetic mixture were chosen to be the tunable parameters. A random number generator provided the starting points for the optimization algorithm. The exact values of the critical temperature of the second, third and fourth component are 469.6 K, 622.1 and 782.9 K respectively. Table 7.6 shows the optimized values obtained after the tuning process and it can be observed that they match the real ones.

Table 7.6: Optimized value of critical temperature of the second, third and fourth component in the fifth case scenario.

Type	Number	Exact Value	min	max	Optimized Value
Tc	2	469.60	375.68	563.52	469.52
	3	622.10	450.00	700.00	622.23
	4	782.90	520.00	900.00	782.97

7.1.6 Sixth Case Scenario – Synthetic mixture

In the fifth case scenario, the critical pressure, critical temperature and acentric factor of the fourth component of the synthetic mixture were chosen to be the tunable parameters. A random number generator provided the starting points for the optimization algorithm. The real values of the critical pressure, the critical temperature and the acentric factor of the fourth component are 1.4550 MPa, 782.9 K and 0.816053 respectively. Table 7.7 shows the optimized values obtained after tuning and it can be observed that they are very close to the real ones.

Table 7.7: Optimized value of the critical pressure, the critical temperature and the acentric factor of the fourth component in the sixth case scenario.

Type	Number	Exact Value	min	max	Optimized Value
Pc	4	1.455	1.000	1.600	1.430
Tc	4	782.90	600.00	939.00	769.89
Omega	4	0.816	0.600	0.900	0.871

At this point, it is worth mentioning that a human is not able to comprehend the four dimension space, a fact that renders visualization in the 4D space not possible. One way to visualize the multivariable function of the sixth case scenario is by assuming that the value of one of the three independent variables, for instance the acentric factor's value, is constant at a certain value. Then it is possible to create a contour plot where the two independent variables are the critical pressure and the critical temperature of the fourth component, the dependent variable is the objective variable and the acentric factor has a constant value, i.e. 0.7. However, the global minimum observed will not be the real global minimum of the objective function but rather the minimum of the objective function given that the acentric factor of the fourth component is equal to 0.7 (cross section contour plot).

7.2 Real reservoir fluid 1

As soon as it was established that the optimizer developed in Matlab is efficient for the simple four-component synthetic mixture, the optimizer was tested on a real reservoir fluid. This fluid is difficult to be tuned as it is very volatile, which means that the pressure path in the reservoir is closer to the critical conditions. Table 7.8 depicts the composition of the real reservoir fluid before the split and lump of the hydrocarbon plus fraction.

Table 7.8: Composition of the real reservoir fluid 1 before split and lump.

Component	Composition (%)
N ₂	0.1
CO ₂	0.7
C ₁	53.3
C ₂	6.7
C ₃	4.8
i - C ₄	0.7
n - C ₄	2.2
i - C ₅	0.8
n - C ₅	1.9
C ₆	3.3
C ₇	4.5
C ₈	4.6
C ₉	3.4
C ₁₀	2.2
C ₁₁	1.7
C ₁₂₊	9.1

The CCE and DLE experiments were simulated using the CCE and DLE simulators developed in Matlab and the estimations were compared with the corresponding laboratory data. In order for the objective function to be minimized, seven different case scenarios were developed, in each one of which different parameters were selected as the tunable ones. The weight factors used during optimization were set equal to unity for all properties, except for the weight factor corresponding to compressibility, which was set equal to zero. The results received are depicted in Table 7.9. During the tuning process, it was confirmed in each case scenario developed for the real reservoir fluid the optimizer conducted global optimization. It is worth mentioning that the objective function is not convex but has multiple local minima and that the WinProp values are not displayed as they are not the optimal ones.

Table 7.9: Results received after the tuning process before splitting and lumping of the C_{12+} .

First			
Type	Number	Optimized	error
Tc	C_{11}	729.00	0.15
	C_{12+}	849.00	
Second			
Type	Number	Optimized	error
Tc	C_{10}	632.28	
	C_{11}	729.47	0.14
	C_{12+}	846.69	
Third			
Type	Number	Optimized	error
Omega	C_{11}	0.700	0.18
	C_{12+}	1.020	
Fourth			
Type	Number	Optimized	error
Pc	C_{12+}	1.075	0.22
Fifth			
Type	Number	Optimized	error
Pc	C_{10}	2.445	
	C_{11}	1.751	0.20
	C_{12+}	1.098	
Sixth			
Type	Number	Optimized	error
Pc	C_{12+}	1.121	
Tc	C_{12+}	930.44	0.14
Omega	C_{12+}	0.73	
Seventh			
Type	Number	Optimized	error
Pc	C_{11}	2.446	
Tc	C_{11}	729.00	
Omega	C_{11}	0.699	
Pc	C_{12+}	1.121	0.13
Tc	C_{12+}	917.05	
Omega	C_{12+}	0.726	

As can be seen in Table 7.9, the “lowest” error is obtained in the seventh case scenario, which is a superset of the first, third, fourth and sixth case scenario. This confirms the globality of the pattern search method as the optimization algorithm is not trapped in a local minimum and takes advantage of the fact that more parameters are selected to be tuned. An interpretation of the results of the case scenarios that are subsets of the seventh case scenario follows.

Table 7.10 depicts the results of the tuning in the first case scenario. As can be seen in Table 7.10, the density of the oil at the bubble point before and after the tuning process has not changed significantly. This is to be expected as the volume shift of all components is set equal to zero before tuning and is not adjusted during the tuning process. As far as the saturation pressure is concerned, the value assigned to it after the optimization cannot be deemed as adequate. The optimizer is not that efficient in matching the estimated saturation pressure with the laboratory one due to the weight factor of the saturation pressure being set equal to unity. Finally, the value assigned to B_o at the bubble point is satisfactory even though B_o is a function of density. This can be explained by the cancellation of errors that takes place.

Table 7.10: First case scenario.

Before Tuning		After Tuning		Lab
$P_{sat}@P_b$ (MPa)	31.81	$P_{sat}@P_b$ (MPa)	29.87	26.77
$B_o@P_b$	2.180	$B_o@P_b$	2.040	1.970
$\rho@P_b$ (g/cm ³)	567.00	$\rho@P_b$ (g/cm ³)	566.00	586.00

Table 7.11 depicts the results of the tuning in the third case scenario. In the third case scenario, the error after the optimization is 0.176 (Table 7.9) and it is greater than the corresponding one in the first case scenario, which is equal to 0.1457. This is to be expected because the effect that the acentric factor has on the total error is significantly less than the effect of the P_c and T_c on the total error of the objective function.

Table 7.11: Third case scenario.

Before Tuning		After Tuning		Lab
$P_{sat}@P_b$ (MPa)	24.75	$P_{sat}@P_b$ (MPa)	29.83	26.77
$B_o@P_b$	2.130	$B_o@P_b$	2.070	1.967
$\rho@P_b$ (g/cm ³)	551.00	$\rho@P_b$ (g/cm ³)	572.00	586.00

Table 7.12 depicts the results of the tuning in the fourth case scenario. As can be seen in Table 7.12, the value of the saturation pressure after the tuning process is close to the laboratory one even though the weight factor of the saturation pressure is one. This is because of the fact that P_c has a strong effect on the saturation pressure.

Table 7.12: Fourth case scenario.

Before Tuning		After Tuning		Lab
$P_{sat}@P_b$ (MPa)	40.49	$P_{sat}@P_b$ (MPa)	27.64	26.77
$B_o@P_b$	2.260	$B_o@P_b$	2.090	1.967
$\rho@P_b$ (g/cm ³)	667.00	$\rho@P_b$ (g/cm ³)	561.00	586.00

Table 7.13 depicts the results of the tuning in the sixth case scenario. As can be seen in Table 7.13, the global optimizer improved significantly the density of the oil and the B_o value at the bubble point.

Table 7.13: Sixth case scenario.

Before Tuning		After Tuning		Lab
$P_{sat}@P_b$ (MPa)	24.506	$P_{sat}@P_b$ (MPa)	29.036	26.770
$B_o@P_b$	2.540	$B_o@P_b$	2.020	1.967
$\rho@P_b$ (g/cm ³)	628.00	$\rho@P_b$ (g/cm ³)	553.00	586.00

7.3 Real reservoir fluid 2

In the last part of this study, the optimizer was tested on the real reservoir fluid 2 after the splitting and lumping of the heavy fraction was applied. The composition of the real reservoir fluid 2 after the split and lump of the C_{7+} is depicted in Table 7.14. This fluid was selected due to its high concentration in H_2S .

Table 7.14: Composition of the real reservoir fluid 2 after split and lump.

Component	Composition (%)
N_2	0.34
CO_2	3.40
H_2S	40.75
C_1	6.56
C_2	2.60
C_3	4.34
i - C_4	1.11
n - C_4	2.57
i - C_5	1.85
n - C_5	1.70
C_6	3.40
F_1	14.04
F_2	13.74
F_3	3.60

The CCE and DLE experiments as well as the separator test were simulated using the CCE, DLE and ST simulators developed in Matlab and the estimations were compared with the corresponding laboratory data. In order for the objective function to be minimized, the critical pressure, the critical temperature, the acentric factor and the volume shift of F_1 and F_2 were selected to be tuned. In addition, the binary interaction coefficients of C_1 and F_1 , C_1 and F_2 , H_2S and F_1 , and H_2S and F_2 were also selected as tunable parameters.

After the Matlab optimization process was completed, the estimations of the PR EoS were plotted against pressure. At the same plot, the estimations of the PR EoS after the tuning process which was performed in CMG’s WinProp (gradient-based optimizer) were also plotted against pressure in an attempt to investigate which optimizer is more efficient.

In the next part of this section, the results, obtained after the tuning process of the PR EoS parameters and the simulation of the laboratory tests for the real reservoir fluid, are presented.

Saturation pressure

As can be seen in Table 7.15, both PR EoS models, the one tuned by the Matlab optimizer and the EoS model whose parameters were optimized by the CMG optimizer, are efficient in matching the laboratory saturation pressure.

Table 7.15: Saturation pressure after the optimization process.

	Lab	Matlab	CMG
Saturation Pressure (psia)	1,189.7	1,189.7	1,189.7

Constant composition expansion (CCE)

In the case of the constant composition expansion test, the physical properties to be evaluated are the relative oil volume (V_r) and the isothermal compressibility within the range of pressures above the bubble point pressure.

Relative volume

As can be seen in Figure 7.5, after the tuning process of the PR EoS in Matlab and WinProp, the estimations are very close to the laboratory ones.

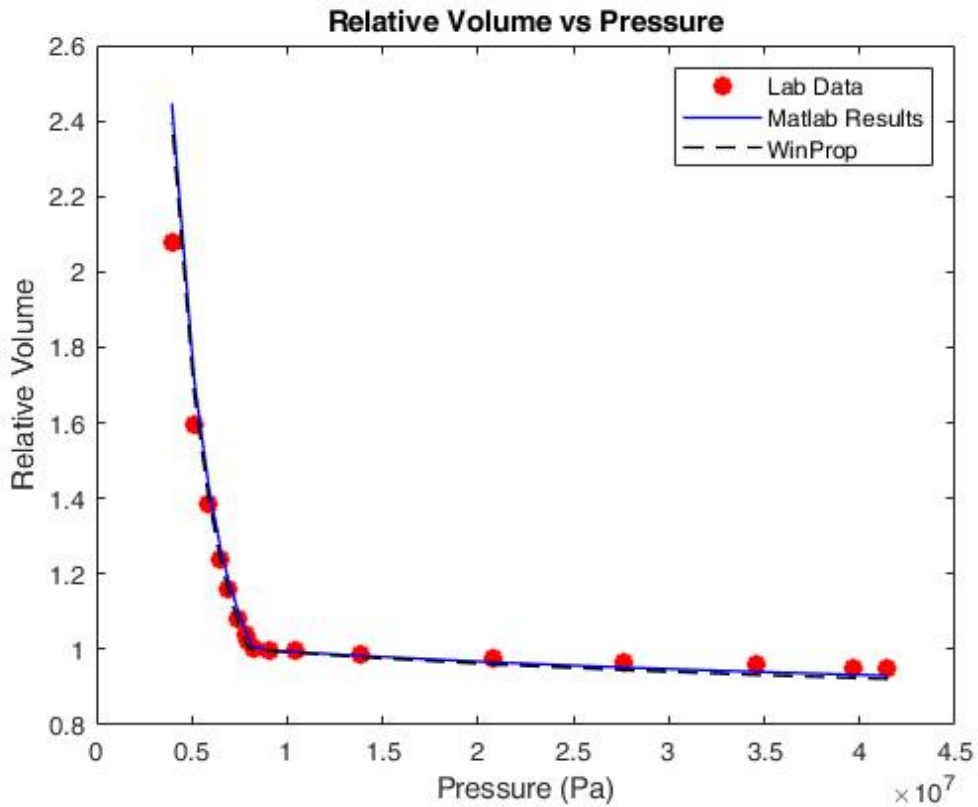


Figure 7.5: Relative Volume vs Pressure.

Isothermal compressibility

The isothermal compressibility estimations are considered acceptable as the PR EoS models after the adjustment of the tunable parameters using the Matlab. In any case, it is emphasized that the compressibility of this fluid exhibits very low value, despite the volatility of the fluid, which means that small differences between the PR EoS's estimations and the laboratory data, can result in large relative deviations, which however do not affect significantly the accuracy of the EoS model.

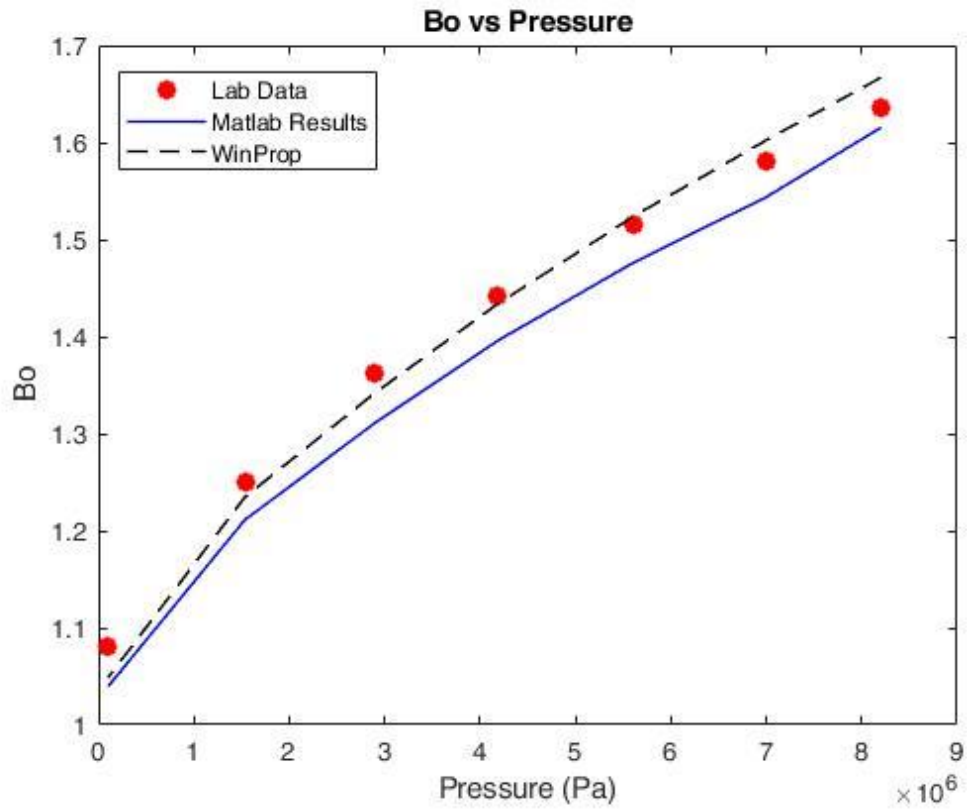


Figure 7.7: B_o vs Pressure.

Solution Gas Oil Ratio (R_s)

Figure 7.8 shows that the two PR EoS models, the one that was tuned by the Matlab optimizer and the one tuned by the WinProp optimizer, both describe R_s in the diphasic region very accurately. However, the Matlab EoS model can be deemed as slightly more efficient.

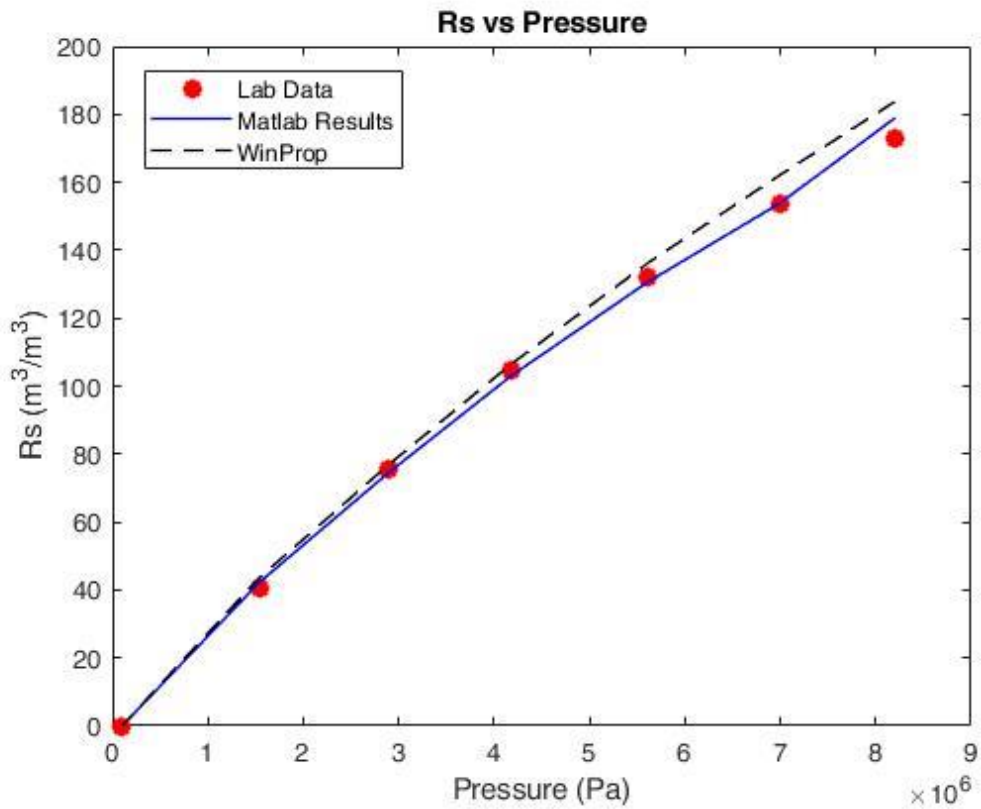


Figure 7.8: R_s vs Pressure.

Oil density

Figure 7.9 shows that the PR EoS model tuned by the Matlab describes oil density in the diphasic region very accurately. This is to be expected as the volume shifts of F_1 and F_2 were tuned. It is worth noticing that the Matlab EoS model can be deemed as more efficient than the WinProp one.

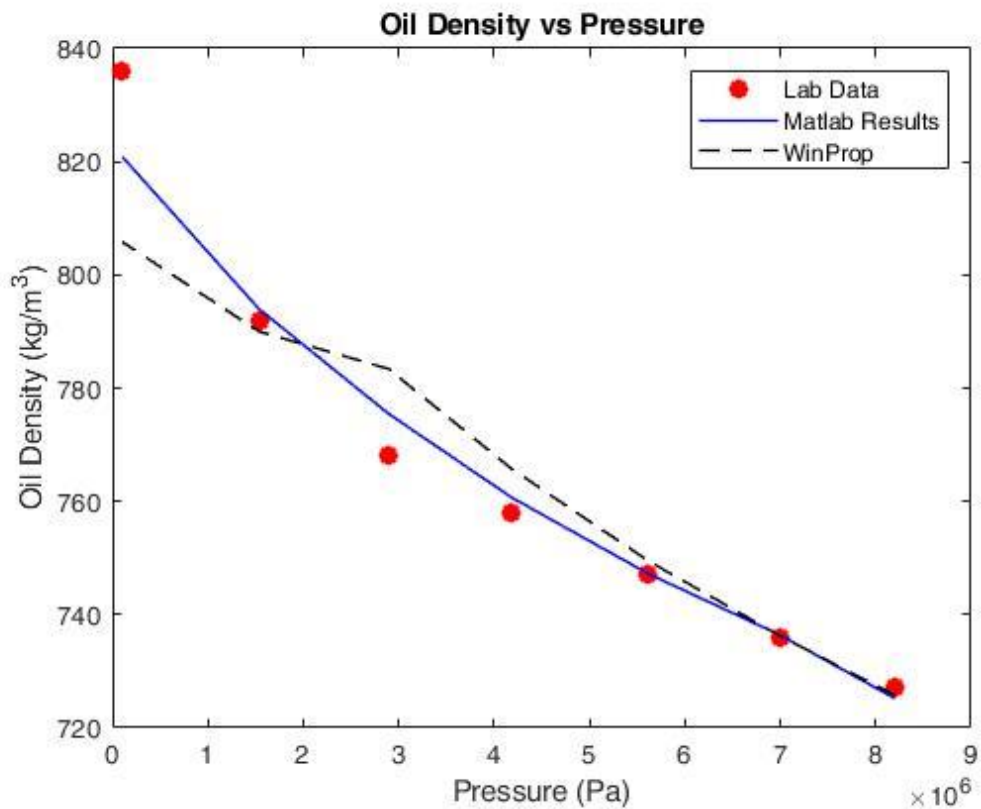


Figure 7.9: Oil density vs Pressure.

Compressibility factor (Z)

Figure 7.10 shows that the two PR EoS models, the one that was tuned by the Matlab optimizer and the one tuned by the WinProp optimizer, both describe the Z factor in the biphasic region very accurately. It is worth noticing that, at atmospheric pressure (101,352 Pa), a big deviation between the lab data and the EoS models' estimations can be observed as the latter provides a value of 0.97 as opposed to the naturally occurring $Z = 1$.

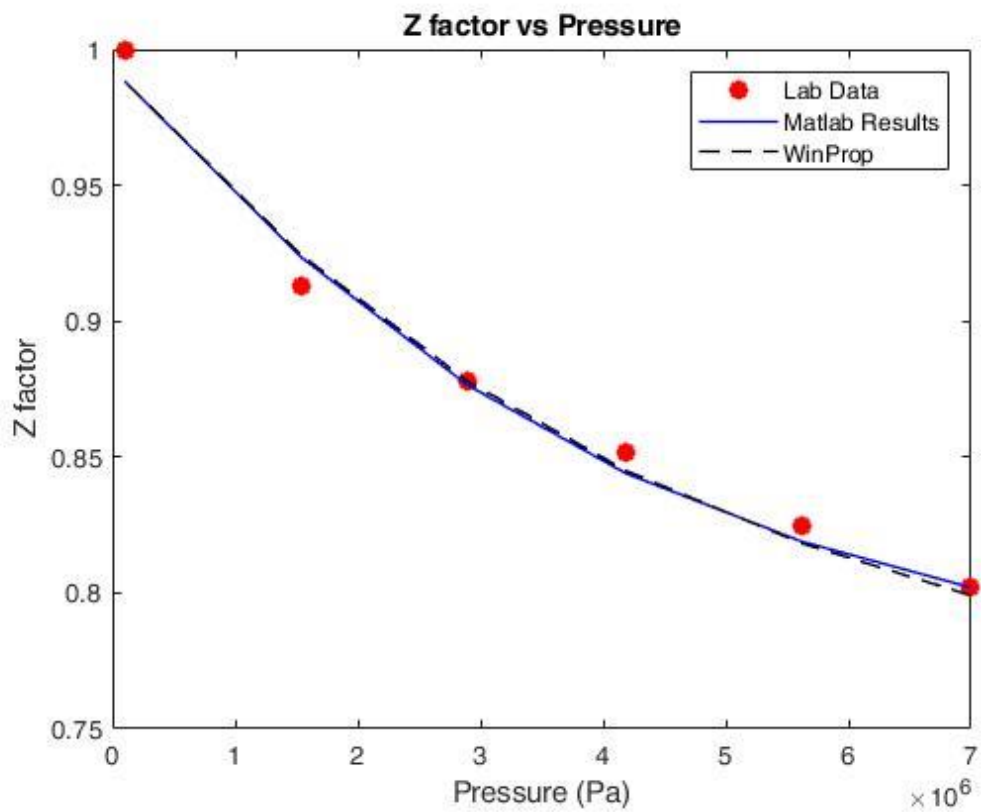


Figure 7.10: Z factor vs Pressure.

Specific gravity of gas (S_g)

Figure 7.11 shows that the two PR EoS models, the one that was tuned by the Matlab optimizer and the one tuned by the WinProp optimizer, both describe the specific gravity of gas in the biphasic region very accurately. It is worth noticing that, in the atmospheric pressure (101,352 Pa), a big deviation between the lab data and the EoS models' estimations can be observed, thus implying a strong mismatch of the released gas composition.

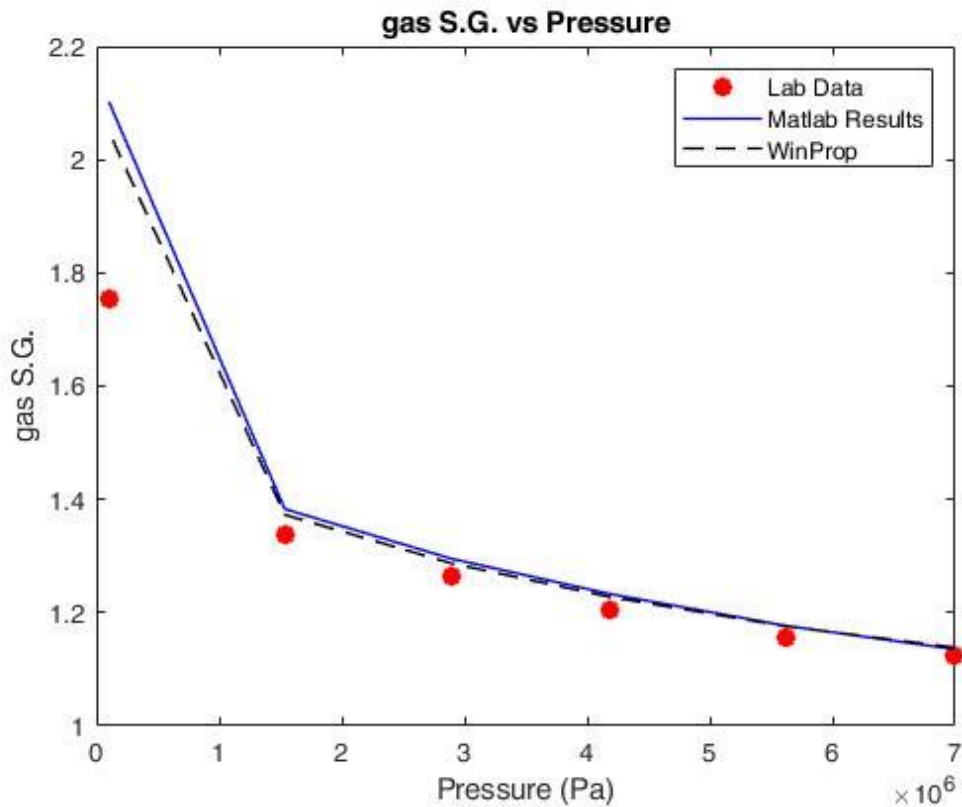


Figure 7.11: S_g vs Pressure.

Separator test

In the case of the Separator test, the properties that are evaluated are the:

- Gas Oil Ratio (GOR)
- API

As can be seen in Table 7.16, the EoS model tuned using the Matlab optimizer yields significantly better results compared to the commercial software. It is worth mentioning that it took the operator a huge amount of time to come up with these results using CMG's WinProp.

Table 7.16: Separator Test Results.

	Lab Data	Matlab	WinProp
GOR (scf/stb)	649	673.02	809.71
API	28.75	30.15	34.02

8. Conclusions

It is well known that one of the main drawbacks of the gradient-based optimization methods is that global optimality cannot be easily guaranteed. The tuning procedure of an Equation of State model is significantly complex since it requires the minimization of a highly nonlinear and non-convex objective function. It is apparent that optimizing such a function can be quite challenging. This is the reason why the pattern search method, which is a global optimization method that can be used on functions that are not differentiable and has a wider viewing angle as far as the global minimum is concerned, was selected. The globality of the employed method was confirmed by the fact that the pattern search method improves the value of the multivariate objective function when more parameters were selected to be tuned.

Regarding the accuracy and physical soundness of the estimations of the tuned Equation of State model, these were guaranteed as the developed tuning algorithm is flexible and allows physical constraints concerning the nature of the components to be imposed rather than solely box constraints as it happens in the case of the WinProp software.

Finally yet importantly, it was found that assigning appropriate values to the weighting factors of the properties is one of the most important prerequisites of the tuning procedure. At this point, it is important to mention that it is not possible to match all laboratory observations with equal accuracy.

To conclude, this optimization method proves to be competitive in terms of its performance and ability to track global solutions while providing simultaneously physically sounded estimations.

References

- Agarwal, R. L.-K. (1987). *"A Regression Technique with Dynamic-Parameter"*.
- Aguilar, R., & McCain, W. (2002). An Efficient Tuning Strategy to Calibrate Cubic EoS for Compositional Simulation. *SPE*.
- Ahmed, T. (2016). *Equations of State and PVT Analysis*. Cambridge, USA: Gulf Professional Publishing.
- Al-Meshari, A. (2005). *New Strategic Method To Tune Equation-of-State To Match Experimental Data For Compositional Simulation*. Texas: Ph.D. Dissertation.
- Christensen, P. (1999). Regression to experimental PVT data. *J. Can. Petroleum Technol.*, 1-9.
- Coats, K., & Smart, G. (1986). Application of a Regression-Based EOS PVT Program to Laboratory Data. *SPE*, 277-299.
- Danesh, A. (1998). *PVT AND PHASE BEHAVIOUR OF PETROLEUM RESERVOIR FLUIDS*. Edinburgh: Elsevier.
- Fanchi, J. R. (2006). *Principles of Applied Reservoir Simulation*. Elsevier.
- Jhaveri, B., & Youngren, G. (1988). Three-parameter modification of the Peng-Robinson. *SPE Reservoir Engineering* 3 (03), 1033-1040.
- Katz, D. L., & Firoozabadi, A. (1978). Predicting phase behavior of condensate/crude-oil systems using methane interaction coefficients. *Petrol. Tech.*, 1649-1655.
- Katz, D., & Firoozabadi, A. (1978). Predicting Phase Behavior of Condensate/Crude-Oil Systems Using Methane Interaction Coefficients. *SPE* .
- Mehra, R. (1981). *The Computation of Multi-Phase Equilibrium in Compositional Reservoir Studies*. University of Calgary.
- Michelsen, M. (1982). THE ISOTHERMAL FLASH PROBLEM . PART I. STABILITY. *Fluid Phase Equilibria*, 1-9.
- Pedersen, K. S., & Christensen, P. L. (2007). *Phase behavior of petroleum reservoir fluids*. Florida: CRC Press.

- Pedersen, K., Thomassen, P., & Fredenslund, A. (1982). *Phase equilibria and separation process*. Denmark: Institute for Kemiteknik, Denmark Tekniske Hojskole.
- Pedersen, K., Thomassen, P., & Fredenslund, A. (1989). Characterization of gas condensate mixtures. *Advances in Thermodynamics*, 137-152.
- Péneloux, A., Rauzy, E., & Fréze, R. (1982). A consistent correction for Redlich-Kwong-Soave. *Fluid Phase Equilibria* 8 (1), 7-23.
- Smith, G. (2013, March 27). Retrieved from PetroWiki: https://petrowiki.org/File:Vol5_Page_0897_Image_0001.png
- Whitson, C. (1980). Characterizing hydrocarbon-plus fractions. *European Offshore Petroleum Conference*, (σσ. 294-296). London.
- Whitson, C. (1983). Characterizing hydrocarbon plus fraction. *Society of Petroleum Engineers Journal*, 683-694.
- Whitson, C. (1984). Effect of C7+ properties on equation-of-state predictions. *Society of Petroleum Engineers Journal* 24 (06), 685-696.
- Whitson, C. (2000). Phase Behavior. *SPE*.
- Σταματάκη, Σ., & Αυλωνίτης, Γ. (2004). *Μηχανική Πετρελαίων*. Αθήνα: Εθνικό Μετσόβιο Πολυτεχνείο.